CHAPTER 3A

Rh(III)-Catalyzed Annulation of 2-Arylimidazo[1,2-*a*]pyridines with Maleimides: Synthesis of 1*H*-Benzo[*e*]pyrido[1',2':1,2]imidazo[4,5-*g*]isoindole-1,3(2*H*)-diones and their Photophysical Studies

3.3A.1 INTRODUCTION

Transition metal-catalyzed C–H activation for the construction of carbon-carbon bonds is the most effective and highly desirable strategy for the direct access of complex structures from readily available materials.[1] Hence, extensive efforts have been devoted to afford the highly functionalized and complex scaffolds in an eco-friendly manner with lower cost and fewer synthetic steps. Although, many tandem-, cascade-, and domino-reactions have proved useful to achieve complex synthetic targets,[2-4] development of C**–**H functionalization/annulation reactions have proved to be an attractive strategies to generate molecular complexity with high regio- and stereoselectivity in organic synthesis.[5-6]

The poor regional selectivity has been addressed by the introduction of directing groups into the substrate to achieve the selective C–H functionalization. The directing group enhanced the concentration of the metal catalyst at *ortho* position resulting in higher reactivity and selectivity for the *ortho* C–H bond. Removal of directing groups is required in some cases. To avoid this, the utilization of the traceless or transient directing group has been explored and attracted considerable attention in the past two decades. To date, various transition metal-catalyzed C–H functionalization has been exclusively explored.[7-13] In particular, Rh(III) has engrossed more attention in the field of C–H activation/ annulation due to its significant features such as high selectivity, reactivity, and compatibility with functional groups.[14-17] Among different annulation reactions, Rh(III)-catalyzed annulation of bifunctional arenes with alkynes or alkenes has been extensively studied.[18-20]

On the other hand, imidazo[1,2-*a*]pyridine and its derivatives have attracted great attention in synthetic chemistry due to their wide range of biological activities.[21-24] Imidazo[1,2-*a*]pyridine scaffolds are present as a core moiety in various commercially available drugs such as zolpidem, alpidem, necopidem, seripidem, and zolimidine **(Figure 3.3A.1)**.[25-27] Likewise, succinimide is the most interesting and important skeleton found in the field of medicinal and organic chemistry. Succinimide scaffold is the central pharmacophore of natural products and pharmaceuticals, such as apremilast, thalidomide, phensuximide, and ethosuximide.[28-30] The succinimide moiety can be readily reduced into the pyrrolidine rings or lactams.[31-32] Thus, the functionalization of imidazo[1,2-*a*]pyridine with the installation of succinimides have been an important area of research. In this context, transition metal-catalyzed annulation of imidazo[1,2-*a*]pyridines have achieved significant attention for the construction of structurally diverse extended π-conjugated

polyheterocycles. The numerous coupling partners with imidazo[1,2-*a*]pyridines have been exclusively explored for the bicyclization reactions.

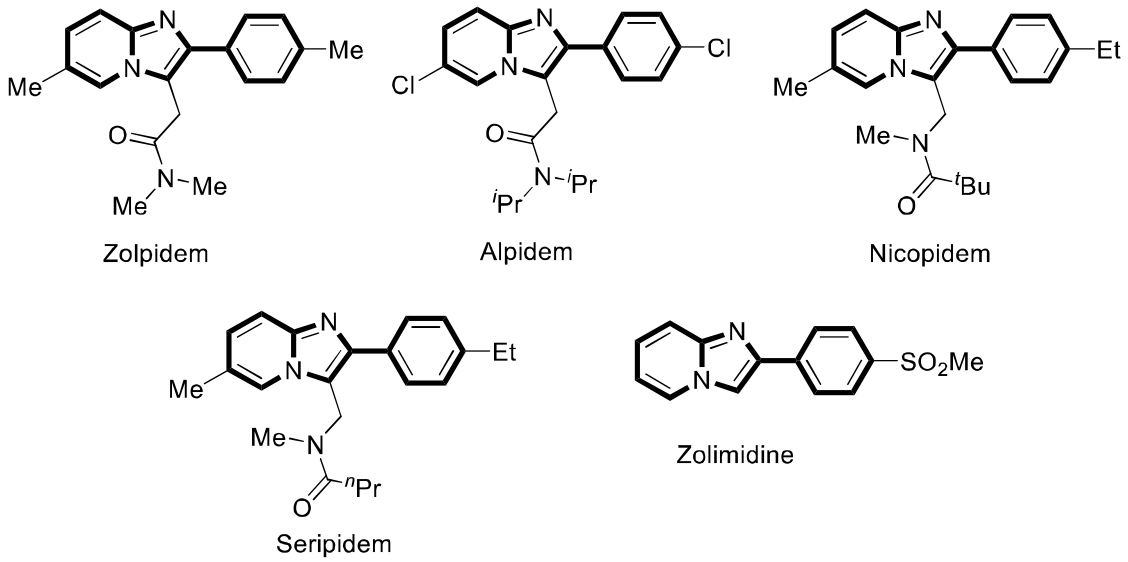

Figure 3.3A.1 Imidazo[1,2-*a*]pyridine based drugs

Fan group developed the palladium(II)-catalyzed oxidative annulation for the synthesis of naphtho[1′,2′:4,5]imidazo[1,2-*a*]-pyridine (NIP) **(3)** and imidazo[5,1,2-*cd*]indolizine (IID) **(4).**[33] The protocol contains the cycloaromatization of imidazo[1,2-*a*]pyridines **(1)** with internal alkynes **(2)** *via* dehydrogenative coupling with a breakdown of the differently located C–H bonds on the 2-phenylimidazo[1,2-*a*]pyridine frameworks. Notably, the reaction displays the broad substrate scope, good functional group compatibility and use of molecular oxygen as oxidant to afford the annulated products in moderate to good yields **(Scheme 3.3A.1)**.

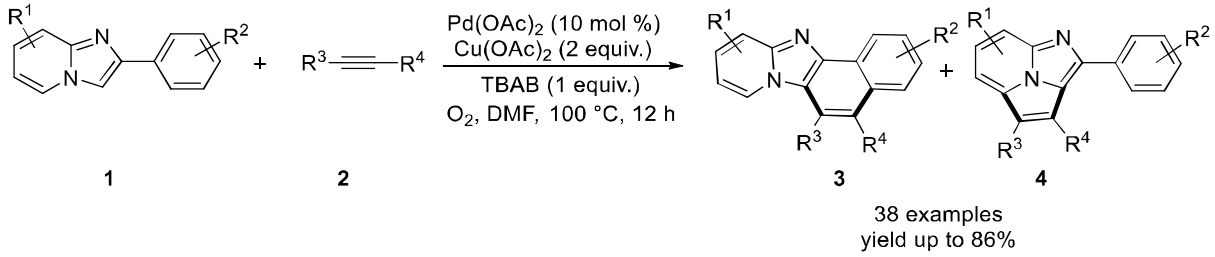

Scheme 3.3A.1. Pd(II)-catalyzed oxidative annulation of imidazo[1,2-*a*]pyridines with alkynes

Similarly, Li and co-workers reported Rh(III)-catalyzed condition controlled two-fold C–H activation of 2-phenylimidazo[1,2-*a*]pyridines **(1)** with substituted alkynes **(2)**.[34] In the presence

of AgOAc, the reaction followed chelation assisted C−H activation pathway at the *ortho* position of phenyl ring and subsequent rollover C−H activation to afford the naphtho-[1′,2′:4,5]imidazo[1,2-*a*]pyridine **(3)** products in good to excellent yields. However, in the presence of $AgBF_4$, the reaction afforded fused isoquinolinium derivatives **(5)** *via* C–C and C–N coupling. The designed strategy was successfully used for the synthesis of extended π-system containing polyazaheterocycles **(Scheme 3.3A.2)**.

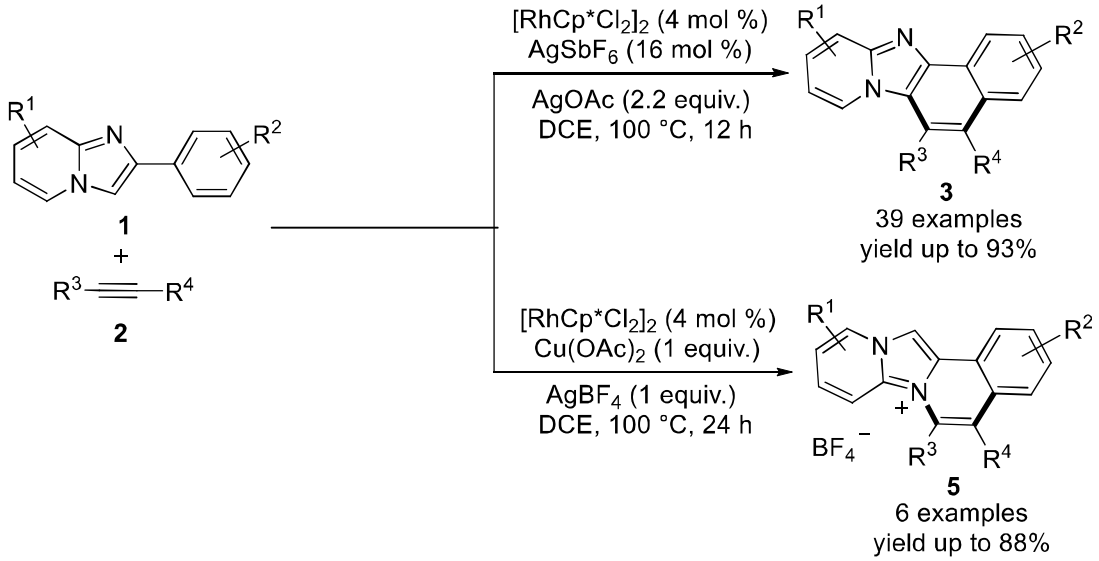

Scheme 3.3A.2. Rh(III)-catalyzed twofold C–H activation of imidazo[1,2-*a*]pyridines with alkynes

In 2015, Cheng *et al*. disclosed the synthesis of naphtho-[1′,2′:4,5]imidazo[1,2-*a*]pyridines **(3)** *via* Rh(III)-catalyzed oxidative annulation reactions between the imidazo[1,2-*a*]pyridines **(1)** with internal alkynes **(2) (Scheme 3.3A.3a)**.[35] This protocol tolerates the large functional groups with moderate to high yields. Verma group reported Rh(III)-catalyzed oxidative dehydrogenative coupling of imidazo[1,2-*a*]pyridines **(1)** with diarylalkynes **(2)** to afford the naphtho[1′,2′:4,5]imidazo[1,2-*a*]pyridines **(3)** in good to excellent yields **(Scheme 3.3A.3b)**.[36] Likewise, Song and co-workers demonstrated the Rh(III)-catalyzed double C–H activation for the construction of naphtho[1′,2′:4,5]imidazo[1,2-*a*]pyridines **(3)** using imidazo[1,2-*a*]pyridines **(1)** with substituted alkynes **(2) (Scheme 3.3A.3c)**.[37] The defined protocol shows some significant features such as short reaction time (2 h), uses $Co(OAc)_2.4H_2O$ as the oxidant under open air and high functional group tolerance. The annulated products displayed deep blue luminescence properties which make them highly susceptible for fluorescent material applications.

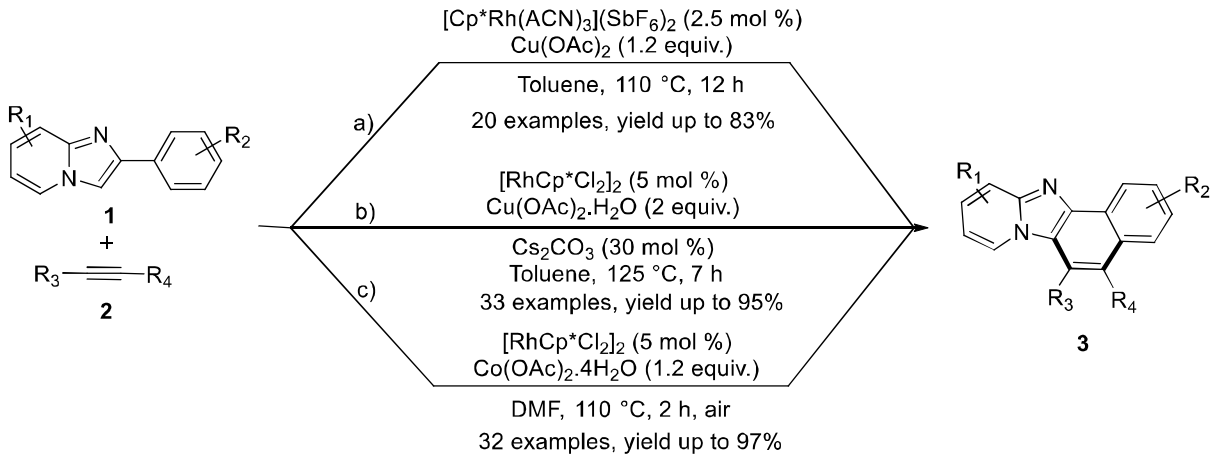

Scheme 3.3A.3 Rh(III)-catalyzed double C–H activation for the synthesis of naphtho-[1′,2′:4,5]imidazo[1,2-*a*]pyridines

Hajra *et al.* reported the palladium(II)-catalyzed dual C–H bond activation using imidazo[1,2-*a*]pyridines **(1)** with diarylalkynes **(2)** to afford the 2,3,4-triarylphenyl-1,7*b*-diaza-cyclopenta[*cd*]indene derivatives **(4)**.[38] The method exhibited high regioselectivity and broad functional groups tolerance with moderate to good yields **(Scheme 3.3A.4)**.

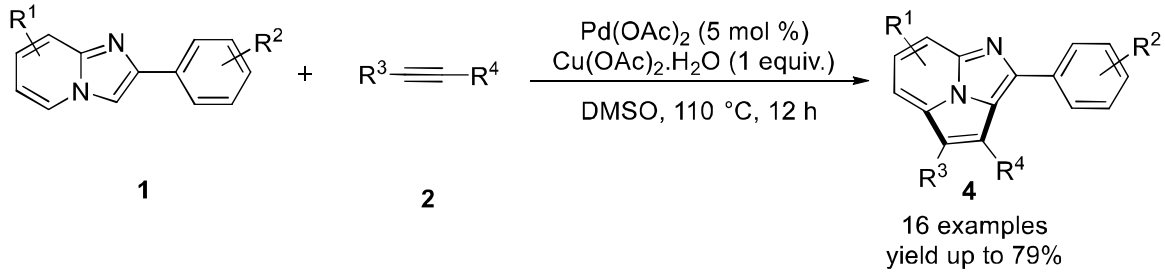

Scheme 3.3A.4 Pd(II)-catalyzed oxidative annulation of imidazo[1,2-*a*]pyridines with alkynes

In 2020, Kumar and co-workers described the site-selective oxidative annulation of 2-phenylimidazo[1,2-*a*]pyridines **(1)** with diarylalkynes **(2)** *via* selenium-coordinated Pd(II) *trans*-dichloride molecular rotor as the catalyst **(Catalyst 1)** for the construction of 2,3,4-triarylphenyl-1,7*b*-diaza-cyclopenta[*cd*]indenes **(4) (Scheme 3.3A.5).**[39] The low-barrier secondary interaction of (SeCH···Cl)-controlled molecular rotor has showed admirable catalytic activity at low catalyst loading (1.5 mol %) with excellent regioselectivity to furnish the annulated products in moderate to good yields.

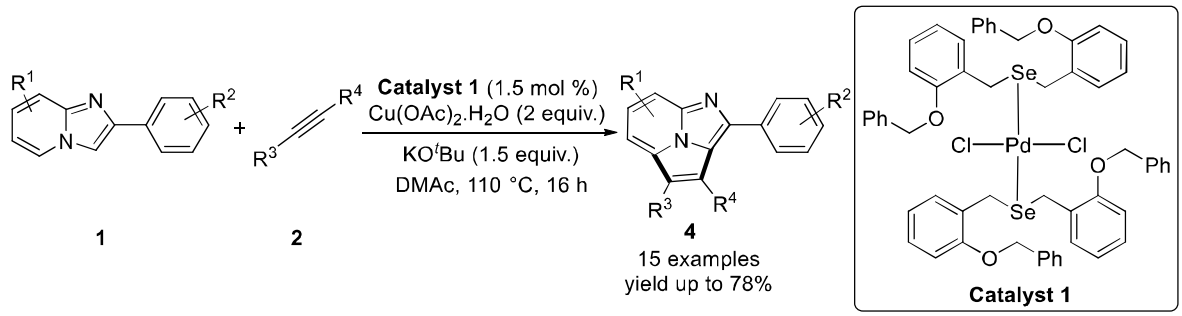

Scheme 3.3A.5 Oxidative annulation of imidazo[1,2-*a*]pyridines with alkynes *via* Pd(II)-catalyzed molecular rotor

Subsequently, Li group explored the Rh(III)-catalyzed annulative coupling between 2-phenylimidazo[1,2-*a*]pyridines **(1)** and sulfoxonium ylides **(6)** for the synthesis of naphtho-[1′,2′:4,5]imidazo[1,2-*a*]pyridines **(7)**.[40] The designed sulfoxonium ylides were used as a bifunctional C_2 synthon, which has been typically utilized in the synthesis of structurally diverse fused hetero- and carbocycles under mild reaction conditions **(Scheme 3.3A.6)**.

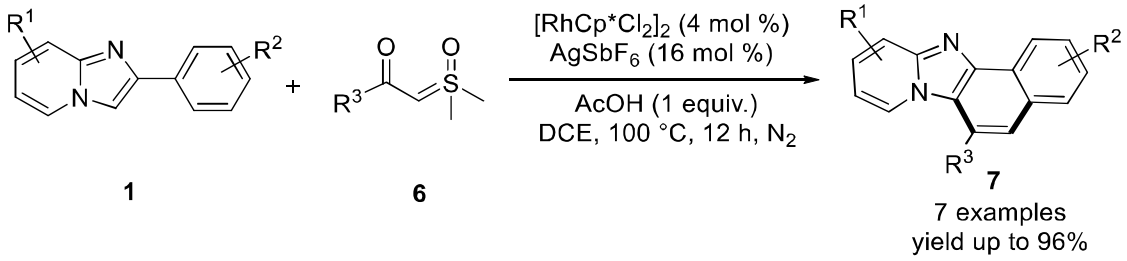

Scheme 3.3A.6 Rh(III)-catalyzed annulative coupling of imidazo[1,2-*a*]pyridines and sulfoxonium ylides

In 2019, Reddy *et al*. elaborated the Rh(III)-catalyzed bicyclizations of imidazo[1,2-*a*]pyridines **(1)** with cyclic enones **(3)** to produce bridged heterocycles **(Scheme 3.3A.7)**.[41] The developed protocol afforded bridged imidazopyridine derivatives **(9)** in good to excellent yields (up to 95%) with high regioselectivity.

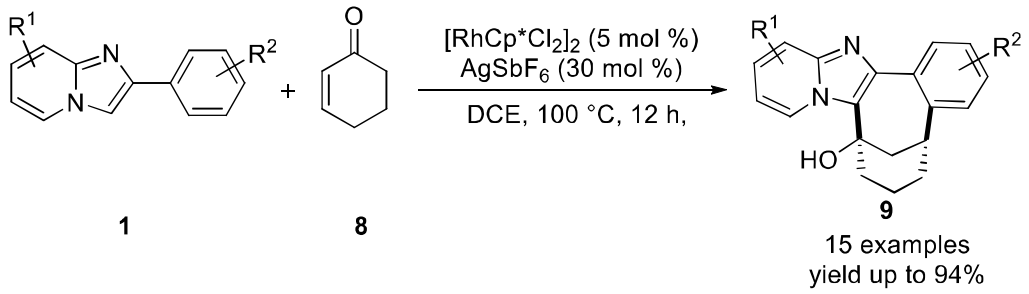

Scheme 3.3A.7 Rh(III)-catalyzed bicyclizations for the synthesis of bridged imidazopyridine compounds

Recently, Miura and co-workers reported the Rh(III)-catalyzed oxidative annulation of 2-phenylimidazo[1,2-*a*]pyridines **(1)** with vinylene carbonate **(10)** to afford the naphtho-[1′,2′:4,5]imidazo[1,2-*a*]pyridines **(11) (Scheme 3.3A.8)**.[42] The designed strategy provides an efficient and straightforward tool for the construction of biologically important polyaromatic scaffolds. The 2-phenylindazoles also tolerate the reaction condition to afford the annulated products in moderate to good yields. The present strategy has shown significant features like no need to external oxidants and bases. Interestingly, the unsubstituted vinylene-fused scaffold could be assembled in single-step operation with high regioselectivity.

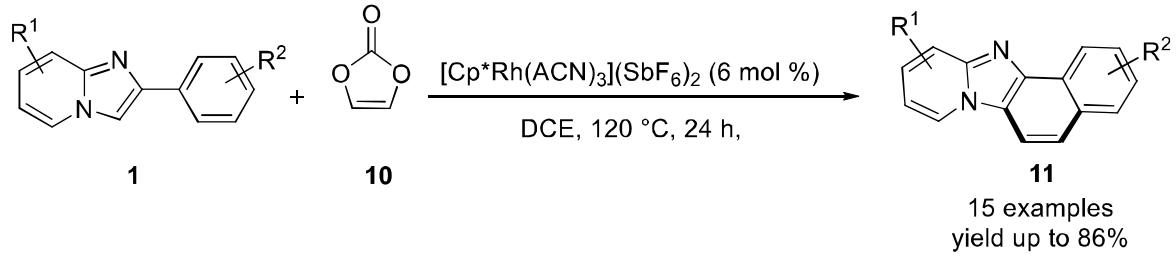

Scheme 3.3A.8 Rh(III)-catalyzed cyclization of 2-phenylimidazo[1,2-*a*]pyridines with vinylene carbonate

Intrigued by pioneering studies on annulation of bifunctional arenes with maleimides and our interest in functionalization of imidazo[1,2-*a*]pyridines, we developed an efficient Rh(III)-catalyzed dehydrogenative annulation of 2-arylimidazo[1,2-*a*]pyridines with maleimides **(Scheme 3.3A.9)**.

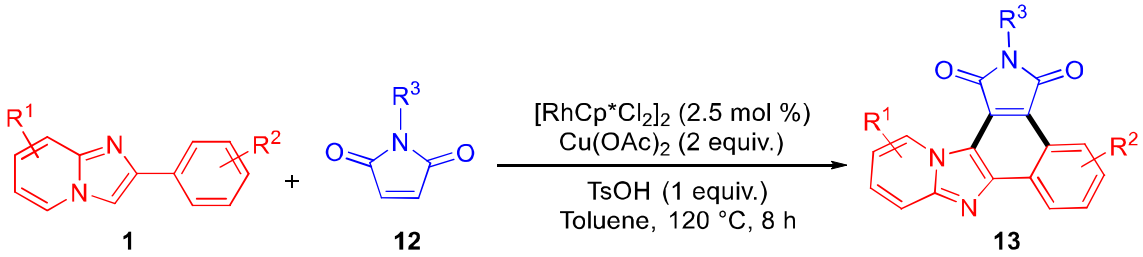

Scheme 3.3A.9 Rh(III)-catalyzed oxidative annulation of 2-phenylimidazo[1,2-*a*]pyridines with maleimides

3.3A.2 RESULTS AND DISCUSSION

Initially, we investigated the model reaction of 2-phenylimidazo[1,2-*a*]pyridine (**1a**), *N*-phenylmaleimide (**12a**), in the presence of $[Cp^*RhCl_2]_2$ (1 mol%), $Cu(OAc)_2$ (2 equiv.) and TsOH (1 equiv.) in toluene at 120 °C for 8 h. To our delight, the annulation product **13aa** was isolated in 78% yield (**Table 3.3A.1**, entry 1). The structure of **13aa** was well established by NMR (^1H, $^{13}C\{1H\}$) and HRMS analysis. On the contrary, yield of **13aa** decreased to 22% on using [Ru(*p*-cymene)$Cl_2]_2$ as catalyst (**Table 3.3A.1**, entry 2) whereas only traces of **13aa** was obtained with $Pd(OAc)_2$ (**Table 3.3A.1**, entry 3). Acidic additives such as 1-adamantane carboxylic acid (ADA), AcOH, and TFA were inferior to TsOH (**Table 3.3A.1**, entries 4-6). Moreover, use of other oxidants such as $Cu(OAc)_2{\cdot}H_2O$, AgOAc, and $Cu(OTf)_2$ were found to be less efficient then $Cu(OAc)_2$ (**Table 3.3A.1**, entries 7-9). Further examination of various solvents such as DCE, CH_3CN, 1,4-dioxane, chlorobenzene, DMF, and HFIP revealed that toluene was most suitable solvent for this annulation reaction (**Table 3.3A.1**, entries 10-15). Thus, $[Cp^*RhCl_2]_2$ (1 mol%), $Cu(OAc)_2$ (2 equiv.) and TsOH (1 equiv.) in toluene at 120 °C for 8 h was eventually chosen as the optimized reaction conditions for subsequent studies of the annulation of 2-arylimidazo[1,2-*a*]pyridines with maleimides. During our work, Fan group and Reddy group also described annulation of maleimides with 2-arylimidazopyridines with $[RhCp^*Cl_2]_2$ and [Ru(*p*-cymene)$Cl_2]_2$ catalyst, respectively.[43-44]

Table 3.3A.1 Optimization of reaction conditions.[a]

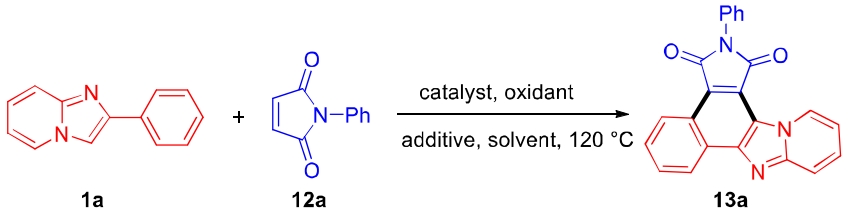

1a 12a 13a

Entry	Catalyst	Oxidant	Additive	Solvent	% Yield[b]
1	$[CpRh^*Cl_2]_2$	$Cu(OAc)_2$	TsOH	Toluene	78
2	$[Ru(p\text{-cymene})Cl_2]_2$	$Cu(OAc)_2$	TsOH	Toluene	22
3	$Pd(OAc)_2$	$Cu(OAc)_2$	TsOH	Toluene	Traces
4	$[Cp^*RhCl_2]_2$	$Cu(OAc)_2$	AdCA	Toluene	47
5	$[Cp^*RhCl_2]_2$	$Cu(OAc)_2$	AcOH	Toluene	63
6	$[Cp^*RhCl_2]_2$	$Cu(OAc)_2$	TFA	Toluene	56
7	$[Cp^*RhCl_2]_2$	$Cu(OAc)_2{\cdot}H_2O$	TsOH	Toluene	69
8	$[Cp^*RhCl_2]_2$	AgOAc	TsOH	Toluene	55
9	$[Cp^*RhCl_2]_2$	$Cu(OTf)_2$	TsOH	Toluene	12
10	$[Cp^*RhCl_2]_2$	$Cu(OAc)_2$	TsOH	DCE	51
11	$[Cp^*RhCl_2]_2$	$Cu(OAc)_2$	TsOH	CH_3CN	57
12	$[Cp^*RhCl_2]_2$	$Cu(OAc)_2$	TsOH	Dioxane	39
13	$[Cp^*RhCl_2]_2$	$Cu(OAc)_2$	TsOH	PhCl	30
14	$[Cp^*RhCl_2]_2$	$Cu(OAc)_2$	TsOH	DMF	16
15	$[Cp^*RhCl_2]_2$	$Cu(OAc)_2$	TsOH	HFIP	5

[a]Reaction conditions: **1a** (0.26 mmol), **12a** (0.39 mmol), catalyst (1 mol %), oxidant (0.52 mmol), additive (0.26 mmol), solvent (2 mL) at 120 °C for 8 h. [b]Isolated yield. TFA = trifluoroacetic acid, AdCA = 1-adamantanecarboxylic acid, DCE = 1,2-dhichloroethane, DMF = *N*,*N*-dimethyl formamide; HFIP = hexafluoroisopropanol.

The structure of the annulated product **13aa** was ascertained by ^1H NMR, $^{13}C\{^1H\}$ NMR and HRMS analysis. In the ^1H NMR of **13aa**, the characteristic peak of C7-H of imidazo[1,2-*a*]pyridine appeared at δ 10.13 ppm and rest of the aromatic protons well matched with the structure **(Figure 3.3A.2)**. In $^{13}C\{^1H\}$ NMR of **13aa**, carbonyl carbon of the *N*-phenyl maleimide appeared at δ 168.59 ppm and δ 167.61 ppm, respectively along with other carbons **(Figure 3.3A.3)**. Finally, peak at *m/z* 364.1061 in the HRMS corresponding to molecular formula $C_{23}H_{14}N_3O_2$ $[M + H]^+$ ion confirmed the structure at **13aa (Figure 3.3A.4)**.

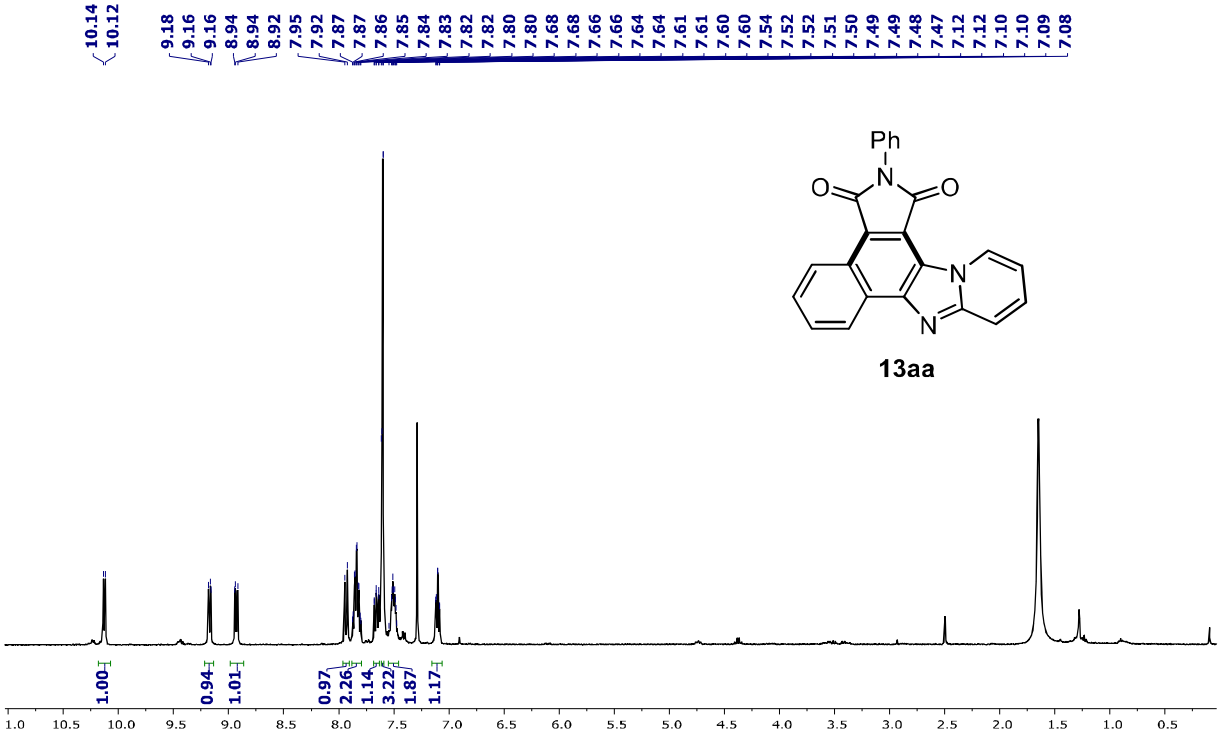

Figure 3.3A.2 ^{1}H NMR spectra of 2-phenyl-1*H*-benzo[*e*]pyrido[1',2':1,2]imidazo[4,5-*g*]isoindole-1,3(2*H*)-dione **(13aa)** in $CDCl_3$

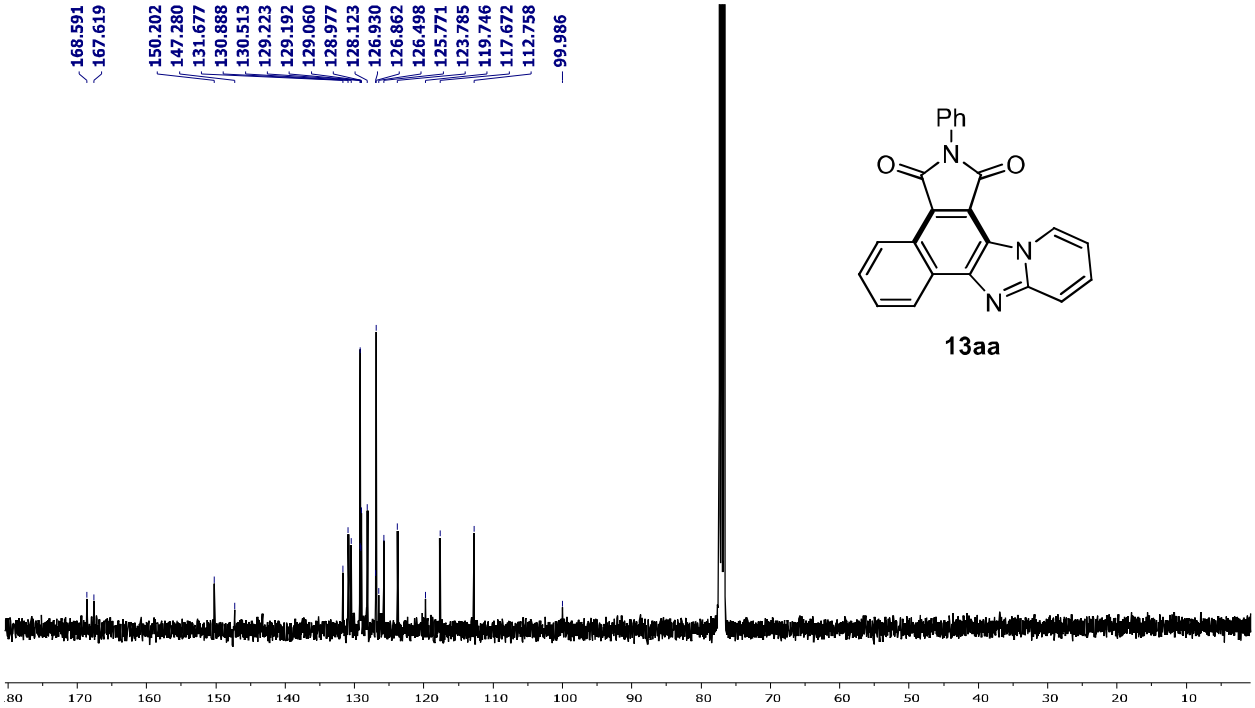

Figure 3.3A.3 $^{13}C\{^{1}H\}$ NMR spectra of 2-phenyl-1*H*-benzo[*e*]pyrido[1',2':1,2]imidazo[4,5-*g*]isoindole-1,3(2*H*)-dione **(13aa)** in $CDCl_3$

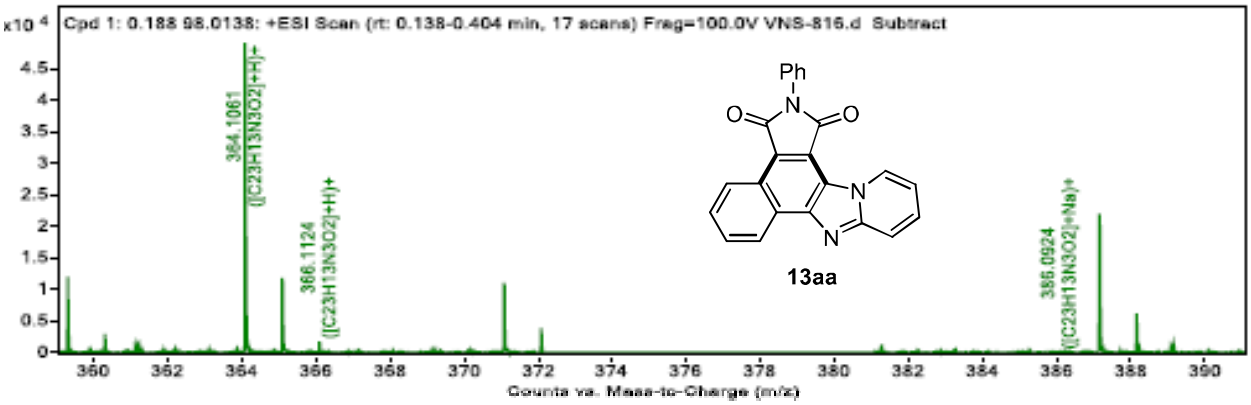

Figure 3.3A.4 HRMS spectrum of 2-phenyl-1*H*-benzo[*e*]pyrido[1',2':1,2]imidazo[4,5-*g*]isoindole-1,3(2*H*)-dione **(13aa)**

Next, we probed substrate scope and generality of the developed annulation reaction **(Table 3.3A.2)**. First, various 2-arylimidazo[1,2-*a*]pyridines (**1a-l**) were selected to realize this annulation reaction with *N*-phenylmaleimide (**12a**). As shown in **table 3.3A.2**, 2-arylimidazo[1,2-*a*]pyridines with electron-donating (**1b**, **1c**) and electron-withdrawing (**1d**, **1e**, **1g**) substituents at the *para*-position of 2-aryl ring underwent smooth annulation to furnish the corresponding annulated products (**13aa–13ga**) in good to excellent yields. Interestingly, slightly higher yields of annulated products were obtained from 2-arylimidazo[1,2-*a*]pyridines with electron-withdrawing substituents at the *para*-position of the 2-aryl ring (**13ba**, **13ca** *vs* **13da**, **13ea**). Dihydro adduct **14ga** was also isolated in 15% yield along with annulated product **13ga** for the reaction of 6-iodo-2-phenylimidazo[1,2-*a*]pyridine (**1g**) with **12a.**

Imidazo[1,2-*a*]pyridines with 2-(naphth-2-yl), 2-(thiophen-2-yl), 2-(thiophen-3-yl) and 2-(2-oxo-*2H*-chromen-3-yl) substituents (**1i-l**) also underwent the C–H annulation reaction with **12a** to give the corresponding annulated products (**13ia–13la**) in good yields (50-71%). It is noteworthy that 6-phenylimidazo[2,1-*b*]thiazole (**1m**) reacted with **12a** under the optimized reaction conditions and produced annulated product **13ma** in a 52% yield. We then probed the generality and substrate scope with respect to various maleimides. Different *N*-substituted maleimides (**12b–12d**) smoothly underwent the annulation reaction with 2-arylimidazo[1,2-*a*]pyridines (**1a-d**) to furnish the corresponding annulated products **13ab–13dd** in moderate to good yields (51-82%). Structure of all the annulated products was confirmed by NMR (^{1}H, ^{13}C{^{1}H}) and HRMS analysis and further, structure of **13ac** was confirmed by single-crystal X-ray diffraction analysis (CCDC no. 1997533) **(Figure 3.3A.5)**.

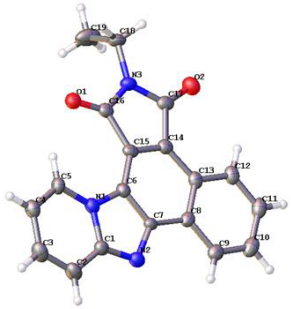

Figure 3.3A.5 Single X-ray crystal structure of **13ac**

Table 3.3A.2 Substrate scope for the synthesis of **13**.[a,b]

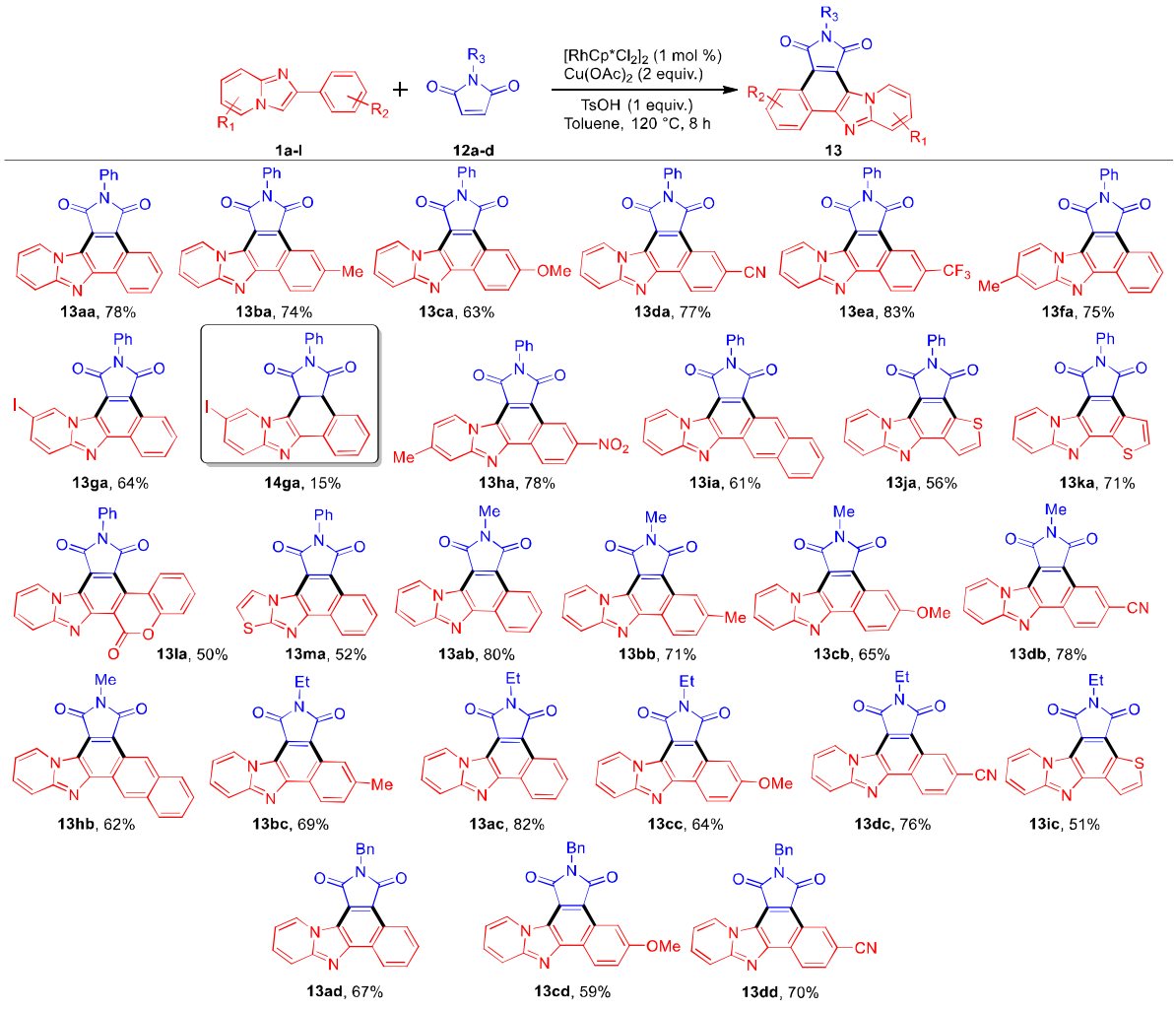

[a]Reaction conditions: **1** (0.26 mmol), **12** (0.39 mmol), $[RhCp^*Cl_2]_2$ (1 mol %), $Cu(OAc)_2$ (0.52 mmol), TsOH (0.26 mmol), Toluene (2 mL) and 120 °C for 8 h. [b]Isolated yield.

To check the practicability and efficiency of the annulation reaction, we carried out the scale-up experiment of **1a** (5.18 mmol) with **12a**. To our delight, the desired annulated product **13aa** was obtained in 73% yield **(Scheme 3.3A.10)**.

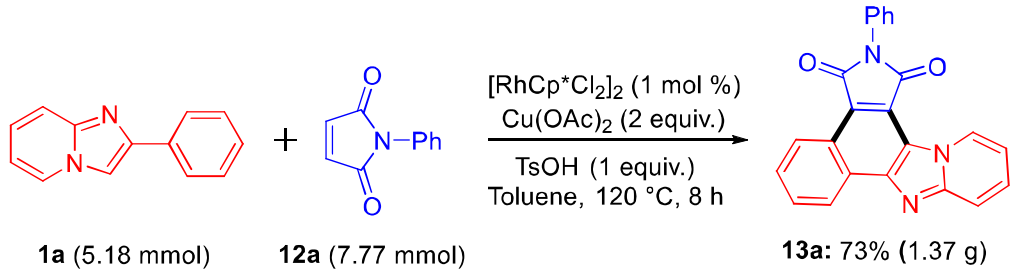

Scheme 3.3A.10 Gram scale experiment

To understand the mode of action a few control experiments were carried out (**Scheme 3.3A.11**). Intermolecular competition experiments with **1a** and **1e** (equimolar mixture) revealed that **1e** with an electron-withdrawing substituent at the *para*-position of the 2-aryl ring reacted preferentially giving **13aa** and **13ea** in the ratio 1:2 **(Scheme 3.3A.11a)**, hence rendering an electrophilic C–H bond activation less likely to be operative. Similarly, intermolecular competition experiment with *N*-phenylmaleimide (**12a**) and *N*-methylmaleimide (**12b**) (equimolar mixture) showed that **12b** reacted preferentially giving **13aa** and **13ab** in the ratio 0.76 : 0.86 **(Scheme 3.3A.11a)**. The presence of 2,2,6,6-tetramethylpiperidine-1-oxy (TEMPO) and butylated hydroxytoluene (BHT) did not affect the outcome of the reaction of **1a** and **12a (Scheme 3.3A.11b)**, thus the possibility of a radical pathway was ruled out. A remarkable D/H exchange (83%) at C(2) position of phenyl ring along with partial D/H exchange (23%) at the C(3) position of imidazo[1,2-*a*]pyridine was observed when **1a** was reacted with $[Cp^*RhCl_2]_2$ (1 mol %), $Cu(OAc)_2$ (2 equiv.), TsOH (1 equiv.) in toluene: D_2O (1: 1 *v/v*, 1 mL) at 120 °C for 8 h **(Scheme 3.3A.11c)**. These H/D exchange results indicate formation of the rhodacycle intermediate **B** in an acetate-assisted, concerted metalation–deprotonation step. A competitive reaction using an equimolar mixture of **1a** and **1a**-d_3 with **12a** revealed a kinetic isotope effect (KIE) of 3.99 (**Scheme 3.3A.11d**), which suggested that phenyl ring C–H activation is the rate-determining step and also supported that a concerted acetate-assisted metalation transition state for C–H activation.[45] The formation of cyclometalated intermediate **B**[34] was also revealed by HRMS analysis of the mixture resulting from the reaction of **1a** in the absence of maleimide (**Scheme 3.3A.11e**)

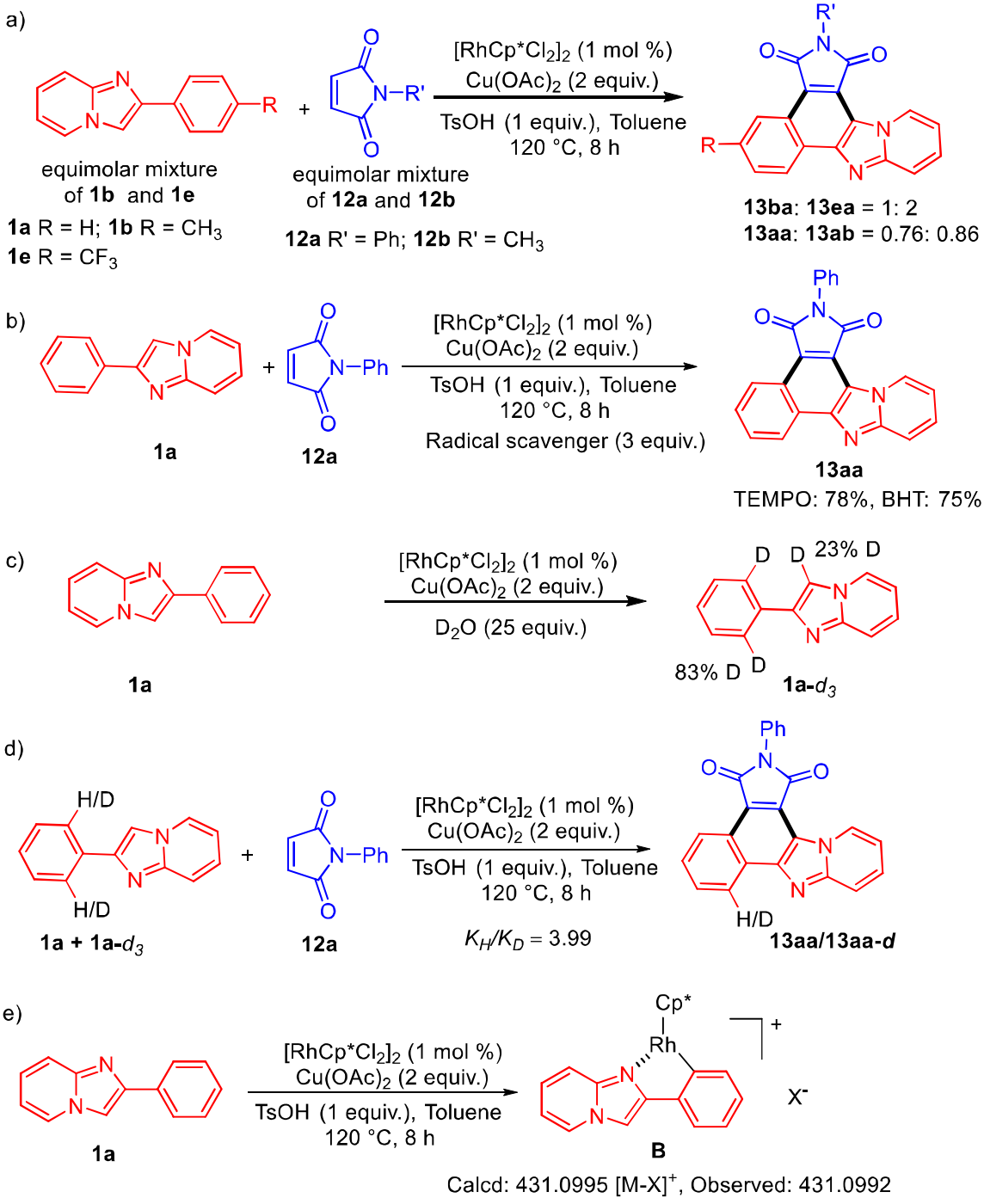

Scheme 3.3A.11 Control experiments

Based on the control experimental results, our own understanding, and previous studies,[34-35, 46-49] a putative mechanism for the annulation reaction is depicted in **Scheme 3.3A.12**. Initially, **1a** coordinates with *in situ* formed active [Cp*RhX$_2$] species to give intermediate **A** which

subsequently undergoes C–H metalation *via* C–H activation to generates rhodacycle **B**. Next, coordination of **12** with rhodacycle **B** followed by migratory insertion affords rhodacycle intermediate **C**. In acidic condition nitrogen de-coordination of **C** and rollover C–H activation affords intermediate **D**. Reductive elimination and protonolysis of intermediate **D** produces intermediate **14** and Rh(I) species. Finally, oxidation of intermediate **14** gives annulated product **13** and oxidation of Rh(I) species by $Cu(OAc)_2$ regenerates the active Rh(III) catalyst.[48-49]

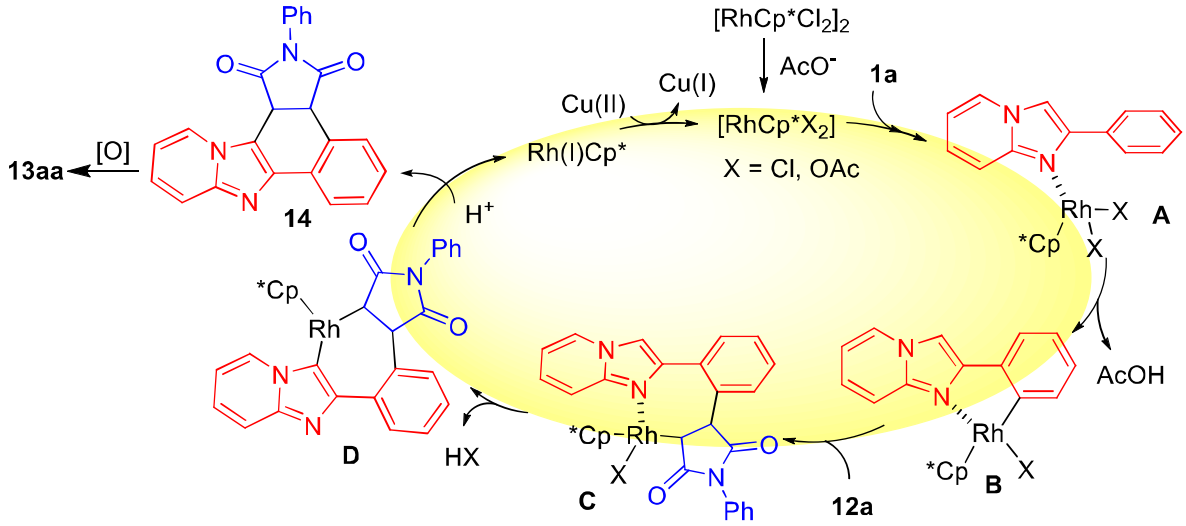

Scheme 3.3A.12 Proposed reaction mechanism

Extended π-conjugated imidazo[1,2-*a*]pyridine derivatives have been found to exhibit strong emission with high fluorescence quantum yields.[50-54] Thus, the photophysical properties of annulated products **13aa-13dd** were evaluated by recording their UV-vis absorption and fluorescence spectra in $CHCl_3$ **(Table 3.3A.3** and **Figure 3.3A.6)**. All the annulated compounds exhibited absorption with λ_{max} ($\pi^* \leftarrow \pi$) in the region 419 – 498 nm and strong emission in the visible region at 532 – 618 nm with a large Stokes shift (4383 – 5845 cm^{-1}). The absorption maxima are bathochromically shifted by more than 200 nm versus parent imidazo[1,2-*a*]pyridines (IP) for most of the annulated products

Table 3.3A.3 Photophysical properties of the annulated products **13**:

Compd.	λ_{max} (nm)[a]		Stokes shift	ε^a ($M^{-1}cm^{-1}$)	% $\Phi_F{}^b$
	Absorbance	Emission (exitation)	cm^{-1} (nm)		
1a	321	378 (320)	4697 (57)	2678	0.35
13aa	447	596 (450)	5592 (149)	11,099	23.8
13ba	447	603 (450)	5788 (156)	11,654	28.6
13ca	444	601 (450)	5884 (157)	9447	29.5
13da	447	555 (440)	4353 (108)	2468	4.7
13ea	445	560 (450)	4615 (115)	9656	7.4
13fa	454	618 (450)	5845 (164)	10,604	45.1
13ga	455	576 (450)	4617 (121)	14,221	12.3
13ha	461	601 (450)	5053 (140)	3311	49.7
13ia	447	605 (468)	5842 (158)	10,473	23.4
13ja	430	576 (450)	5895 (146)	10,512	23.3
13ka	436	539 (440)	4383 (103)	10,213	17.8
13la	421	532 (450)	4956 (111)	8173	3.4
13ab	443	562 (460)	4780 (119)	10,646	57.3
13bb	445	579 (450)	5201 (134)	15,839	60.8
13cb	443	565 (440)	4874 (122)	7270	45.8
13db	443	571 (460)	5060 (128)	13,023	51.9
13hb	498	612 (490)	3740 (114)	5036	46.5
13ac	442	578 (450)	5323 (136)	23,900	58.3
13bc	440	574 (455)	5306 (134)	13,553	55.5
13cc	442	570 (450)	5081 (128)	12,063	46.2
13dc	440	572 (450)	5245 (132)	19,748	62.2
13ic	443	560 (550)	4716 (117)	1673	60.3
13ad	444	584 (450)	5399 (140)	27,864	58.1
13cd	441	570 (450)	5132 (129)	18,534	52.0
13dd	443	572 (450)	5091 (129)	13,806	60.3

[a]All spectra measured in $CHCl_3$ solution (1.0×10^{-5} M) at 25 °C.

[b]Quantum yield (±10%) determined relative to quinine sulfate in 0.5 M H_2SO_4 (Φ_F = 0.55).

Absorption and emission spectra of selected annulated compounds are depicted in **Figure 3.3A.6**. The nature of the substituents significantly tuned the optical properties of the annulated products. Electron-donating groups at C(5)-position of the product exhibited red shift compared to that of **13aa**, whereas electron-withdrawing groups at C(5)-position caused a blue shift of the absorption and emission maxima (**Figure 3.3A.6**). Annulated product with naphthyl fused system **13hb** exhibited red shift (λ_{max} = 498 nm) in comparison to **13aa**. The fluorescence quantum yield of annulated products was calculated using quinine sulfate in 0.5 M H_2SO_4 (Φ = 0.55) as the standard. The compounds are highly fluorescent with moderate to high fluorescence quantum yield and the highest value of the fluorescence quantum yield (Φ_F = 0.62) was recorded for **13dc**. *N*-Phenyl substituted products showed lower quantum yields as compare to *N*-alkyl substituted derivatives.

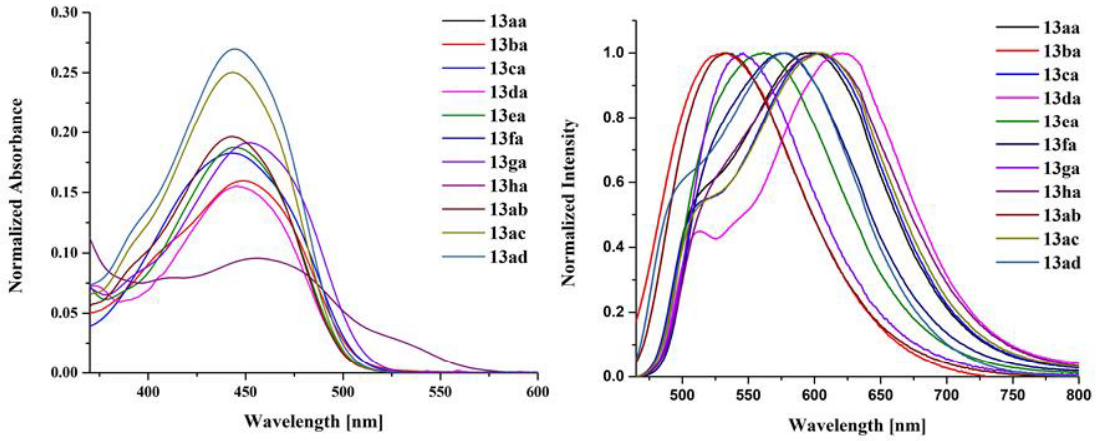

Figure 3.3A.6 UV–vis absorption (left) and normalized emission (right) spectra of a set of annulated compounds (**13aa-ha**, **13ab**, **13ac** & **13ad**) in $CHCl_3$ (1.0×10^{-5} M).

To prove the conjecture about these transitions, time-dependent density functional theory (TD-DFT) was used to calculate the excited states of **13aa** and **13ac** as test cases and visualize the highest occupied molecular orbitals (HOMOs) and lowest unoccupied molecular orbitals (LUMOs) in order to interpret the transitions between them and corresponding transition energies. In this study, we used a long-range-corrected version of B3LYP using the Coulomb-attenuating method (CAM-B3LYP) developed by Handy and co-workers[55] in conjunction with a large 6-311++G(d,p) basis set.[56] Following the experimental condition, $CHCl_3$ is considered as solvent using the integral equation formalism variant (IEFPCM) embedded in the Polarizable Continuum Model (PCM).[57-58] To achieve better numerical accuracy, tight convergence criteria (RMS force threshold = 10^{-5} a.u.) for gradient and *'ultrafine'* numerical grid (99 radial shells and 590 angular

points per atom) were used in the first step. The geometry of **13ac** was extracted from the single crystal structure and **13aa** was built from it. Single point TD-DFT calculations were performed to the ground state equilibrium geometries using the same functionals.

All the calculations were performed using Gaussian 16 software package.[59] **Figure 3.3A.7** shows the computed frontier molecular orbitals (FMOs) for **13aa** and **13ac** molecules. As can be seen, the HOMO of both the molecules is predominantly the π orbitals, with extended π conjugations in the imidazo[1,2-*a*]pyridine moiety and the LUMO are the π* orbitals located in the same region. The computed π* ← π transitions for **13aa** and **13ac** molecules are 413 and 425 nm, respectively which are very close to the experimentally observed values.

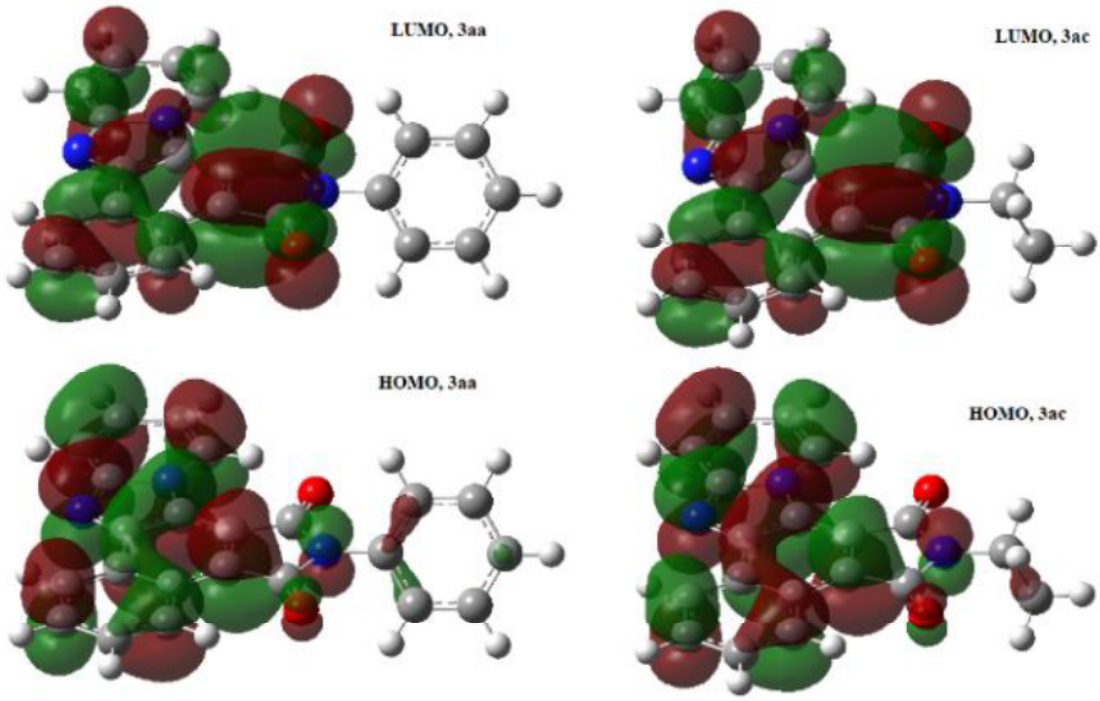

Figure 3.3A.7 Computed frontier molecular orbitals for **13aa** and **13ac**

Next, we investigated the effect of the solvent polarity on the absorption (**Figure 3.3A.8A**) and emission (**Figure 3.3A.8B**) spectra of **13aa**. A redshift in the absorption and emission maxima was observed with an increase in solvent polarity, however, the emission intensity of **13aa** did not decrease in polar solvents. The observed positive solvatochromism may be due to the stabilization of the charge-transfer transition in polar solvents.[60]

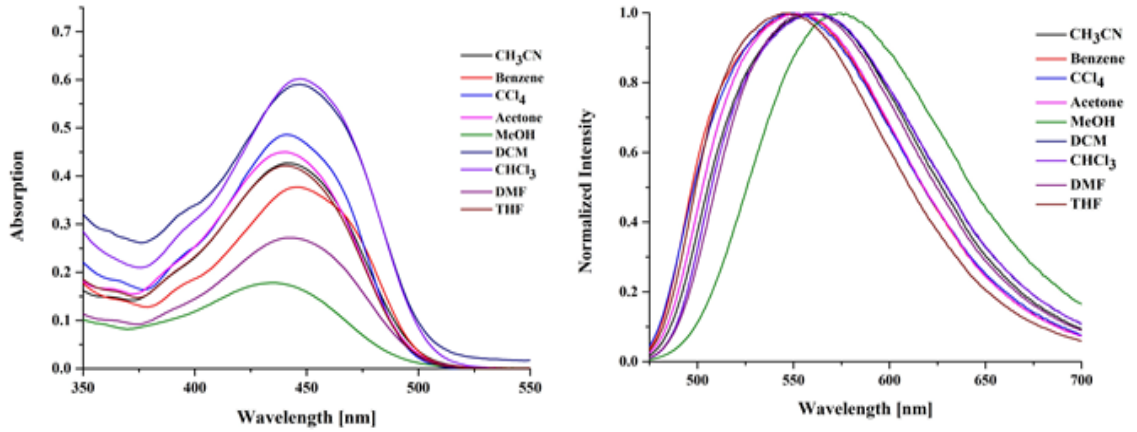

Figure 3.3A.8 A) Absorption and B) normalized fluorescence spectra of **13aa** (1.0×10^{-5} M) in different solvents.

Fused aza-heterocycles have been found to function as a colorimetric and luminescent pH sensor. The nitrogen atom of annulated products had basic character, therefore we investigated absorption and emission spectra of **13aa** as a function of trifluoroacetic acid (TFA) concentration. As can be seen from **Figure 3.3A.9**, significant changes in the absorption and emission spectra of **13aa** in $CHCl_3$ solution were observed upon addition of TFA. The absorption maxima were blue-shifted with the formation of isosbestic points at 418 and 362 nm while emission maxima were red-shifted with gradual decrease in intensity.

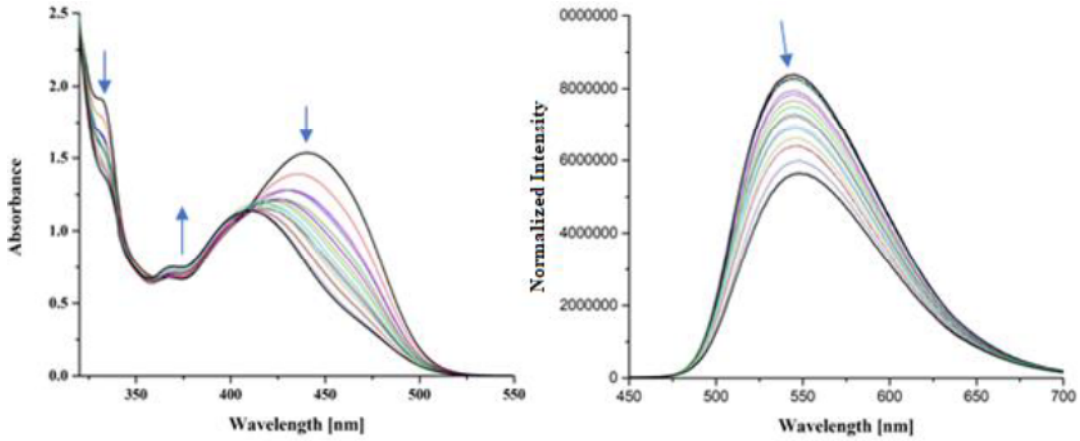

Figure 3.3A.9: A) Absorption and B) fluorescence spectra of **13aa** (1.0×10^{-5} M in $CHCl_3$) in response to addition of TFA from 0 to 0.31 M.

The powdered solids of **13la, 13ja, 13ha,** and **13hb** showed green, yellow, red, and orange fluorescent emission when subjected to ultraviolet (UV) irradiation at 365 nm (**Figure 3.3A.10)**. The results obtained from the photophysical studies implied that annulated products, 1*H*-benzo[*e*]pyrido[1',2':1,2]imidazo[4,5-*g*]isoindole-1,3(2*H*)-diones might be employed as emitting materials in OLED devices.

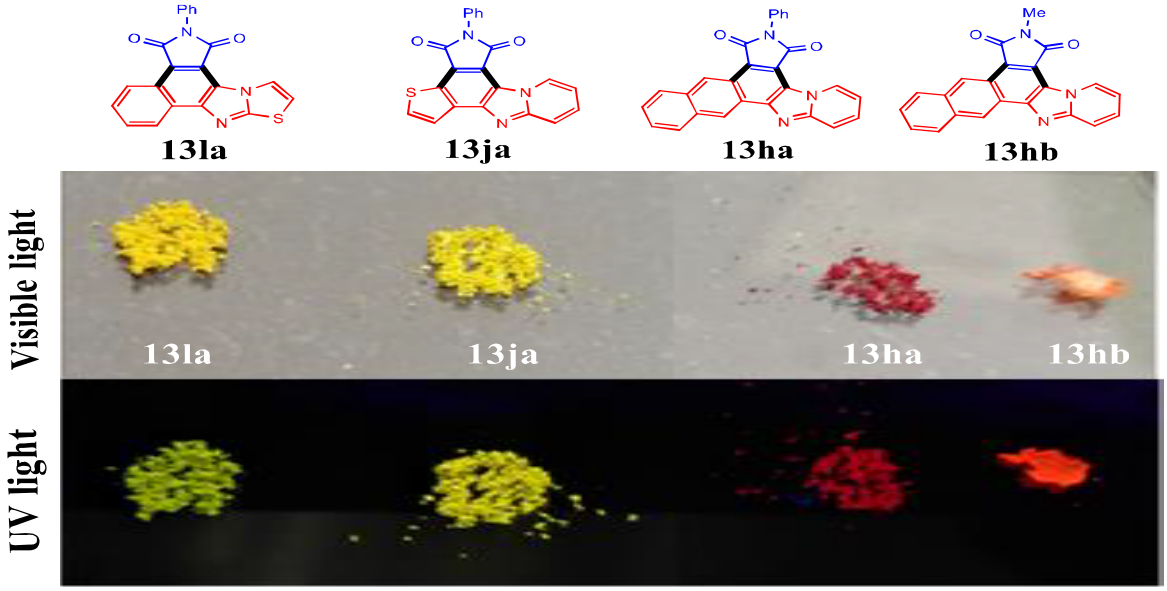

Figure 3.3A.10 Selected illuminant compounds under visible light and UV irradiation at 365 nm

3.3A.3 CONCLUSION

In summary, we have described an efficient Rh(III)-catalyzed annulation of 2-arylimidazo[1,2-*a*]pyridines with maleimides to afford 1*H*-benzo[*e*]pyrido[1',2':1,2]imidazo[4,5-*g*]isoindole-1,3(2*H*)-diones. Different 2-arylimidazo[1,2-*a*]pyridines and maleimides participated well in the reaction to give the corresponding annulated products in good to excellent yields, thus extending the utility of the present method. Absorption and emission spectra of all the annulated products were studied and validated by quantum chemical calculations. All the compounds are highly fluorescent with large Stokes shift and moderate to high fluorescence quantum yield. Compound **13dc** showed the highest (Φ_F = 0.62) fluorescence quantum yield. The emission spectra of **13aa** was red-shifted with increasing solvent polarity with no significant change in fluorescence intensity. The photophysical studies of the annulated products suggest that these compounds might be useful as emitting materials to OLED devices and biosensors.

3.3A.4 EXPERIMENTAL SECTION

3.3A.4.1 General Materials and Methods

All chemicals and solvents were purchased from commercial suppliers and were used without further purification. 2-Arylimidazo[1,2-*a*]pyridines were synthesized by using the procedure reported in the literature.[61] All the reactions were conducted in standard glassware. All the products were purified by column chromatography on silica gel (100-200 mesh). Thin-layer chromatography (TLC) was carried out with a 0.25 mm silica gel 60-F254 plate. Melting points were measured with an automated apparatus and were uncorrected. The ^{1}H and ^{13}C NMR spectra were recorded on a 400 MHz spectrometer with $CDCl_3$ as the solvent and TMS as the internal reference. The coupling constant (J) values are given in Hz, and chemical shift (δ) values are in ppm. The following abbreviations were used for NMR spectra to represent the signal multiplicity: singlet (s), doublet (d), triplet (t), quartet (q), quintet (quint), sextet (sext), septet (sept) and multiplet (m) and their combinations of them as well. HRMS were recorded using the electrospray ionization (ESI) method on a Q-TOF LC-MS spectrometer. All photophysical experiments were performed with spectrophotometric grade DMF, $CHCl_3$, DCM, CCl_4, CH_3CN, THF, benzene, acetone, and deionized H_2O. Relative fluorescence quantum yield (Φ_F) in solution was determined for all compounds **13aa-13dd** by using quinine sulfate in 0.5 M H_2SO_4 (Φ_F = 0.55) as the standard.[62-63]

3.3A.4.2 Experimental Procedure for the Synthesis of Annulated Products (13). A reaction pressure tube equipped with a stir bar was charged with 2-arylimidazo[1,2-*a*]pyridine (**1**, 0.26 mmol), maleimide (**2**, 0.39 mmol), $[RhCp^*Cl_2]_2$ (1 mol %), $Cu(OAc)_2$ (0.52 mmol), TsOH (0.26 mmol) and toluene (2 mL). The resulting mixture was then stirred at 120 °C under air for 8 h. Upon completion, the reaction mixture was cooled down to room temperature, then poured into water, and extracted with EtOAc (10 mL × 3). The combined organic layers were dried over anhydrous Na_2SO_4, and concentrated under reduced pressure. The residue was purified by silica gel chromatography using ethyl acetate/hexane to afford the desired product **13**.

3.3A.4.3 Experimental Procedure for Preparation of 1a-*d*$_3$. 2-Phenylimidazo[1,2-*a*]pyridine (**1a**, 0.26 mmol), $[RhCp^*Cl_2]_2$ (0.0026 mmol), $Cu(OAc)_2$ (0.52 mmol), TsOH (0.26 mmol), D_2O (25 equiv.) and toluene (2 mL) were added to a pressure tube equipped with a stir bar. The resulting mixture was stirred at 120 °C under air for 8 h. After completion of the reaction, the reaction

mixture was poured into water and extracted with ethyl acetate (3 × 10 mL). The combined organic layers were dried over anhydrous Na_2SO_4, and concentrated under reduced pressure. The residue was purified by silica gel chromatography using ethyl acetate/petroleum ether as eluent to give a mixture of **1a** and **1a**-d_3. The mixture was analyzed using ^{1}H NMR spectrometer.

3.3A.4.4 The KIE Studies on 2-Phenylimidazo[1,2-*a*]pyridine. The mixture of **1a** and **1a**-d_3 (0.25 mmol each), **12a** (0.39 mmol), $[RhCp^*Cl_2]_2$ (0.0025 mmol), $Cu(OAc)_2$ (0.5 mmol), TsOH (0.25 mmol) and toluene (3 mL) were charged into a pressure tube. The resulting mixture was then stirred at 120 °C under air for 8 h. After completion of the reaction, the reaction mixture was poured into water and extracted with ethyl acetate (3 × 20 mL). The combined organic layers were dried over anhydrous Na_2SO_4, and concentrated under reduced pressure. The residue was purified by silica gel chromatography using ethyl acetate/petroleum ether as eluent to give a mixture of annulated products **13aa** and **13aa-*d***. The mixture was analyzed using ^{1}H NMR spectrometer and KIE value (k_H/k_D) was found to be 3.99.

2-Phenyl-1*H*-benzo[*e*]pyrido[1',2':1,2]imidazo[4,5-*g*]isoindole-1,3(2*H*)-dione (13aa). Purified

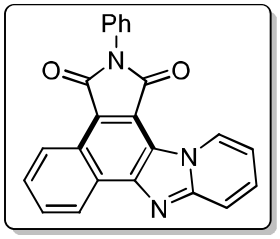

by column chromatography using ethyl acetate/petroleum ether (6: 4 *v/v*) as eluent; yellow solid (73 mg, 78%); mp 268-270 ºC; ^{1}H NMR (400 MHz, $CDCl_3$) δ 10.13 (d, *J* = 7.0 Hz, 1H), 9.18 – 9.16 (m, 1H), 8.94 – 8.92 (m, 1H), 7.93 (d, *J* = 9.2 Hz, 1H), 8.87 – 8.80 (m, 2H), 7.68 – 7.64 (m, 1H), 7.61 – 7.60 (m, 3H), 7.54 – 7.47 (m, 2H), 7.10 (td, *J* = 6.8, 1.3 Hz, 1H); ^{13}C{^{1}H} NMR (100 MHz, $CDCl_3$) δ 168.6, 167.6, 150.2, 147.3, 131.7, 130.9, 130.5, 129.2, 129.2, 129.1, 129.0, 128.1, 126.9, 126.9, 126.5, 125.8, 123.8, 119.8, 117.7, 112.8, 100.0; HRMS (ESI) *m/z*: $[M + H]^+$ calculated for $C_{23}H_{14}N_3O_2^+$, 364.1081; found, 364.1061.

5-Methyl-2-phenyl-1*H*-benzo[*e*]pyrido[1',2':1,2]imidazo[4,5-*g*]isoindole-1,3(2*H*)-dione

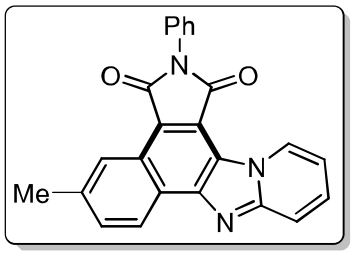

(13ba). Purified by column chromatography using ethyl acetate/petroleum ether (6: 4 *v/v*) as eluent; yellow solid (67 mg, 74%); mp 232-234 ºC; ^{1}H NMR (400 MHz, $CDCl_3$) δ 10.16 (d, *J* = 7.0 Hz, 1H), 9.00 (s, 1H), 8.85 (d, *J* = 8.5 Hz, 1H), 7.94 (d, *J* = 9.2 Hz, 1H), 7.72 (d, *J* = 8.5 Hz, 1H), 7.68 – 7.64 (m, 1H), 7.61 – 7.59 (m, 4H), 7.51 – 7.48 (m, 1H), 7.10 (t, *J* = 8.5 Hz, 1H), 2.68 (s, 3H); ^{13}C{^{1}H} NMR (100 MHz,

$CDCl_3$) δ 168.7, 167.7, 150.2, 140.4, 139.9, 131.8, 131.2, 130.8, 130.5, 129.1, 128.0, 126.8, 126.8, 124.9, 123.6, 120.2, 119.2, 118.8, 117.6, 115.5, 112.6, 22.2; HRMS (ESI) *m/z*: $[M + H]^+$ calculated for $C_{24}H_{16}N_3O_2^+$, 378.1237; found, 378.1188

5-Methoxy-2-phenyl-1*H*-benzo[*e*]pyrido[1',2':1,2]imidazo[4,5-*g*]isoindole-1,3(2*H*)-dione

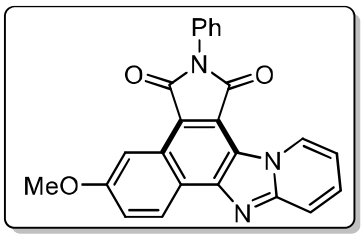

(13ca). Purified by column chromatography using ethyl acetate/petroleum ether (6: 4 *v/v*) as eluent; red solid (55 mg, 63%); mp 305-307 ºC; ^{1}H NMR (400 MHz, $CDCl_3$) δ 10.12 (dt, *J* = 7.0, 1.2 Hz, 1H), 8.82 (d, *J* = 9.2 Hz, 1H), 8.55 (d, *J* = 2.6 Hz, 1H), 7.91 (d, *J* = 9.1 Hz, 1H), 7.66 (ddd, *J* = 9.2, 6.8, 1.3 Hz, 1H), 7.61 – 7.59 (m, 4H), 7.51 – 7.47 (m, 2H), 7.09 (td, *J* = 6.8, 1.2 Hz, 1H), 4.04 (s, 3H); ^{13}C{^{1}H} NMR (100 MHz, $CDCl_3$) δ 168.9, 167.5, 160.4, 150.4, 147.4, 131.7, 131.1, 130.6, 129.2, 128.3, 128.1, 126.8, 125.3, 123.8, 121.5, 120.2, 118.4, 118.2, 117.4, 112.6, 104.1, 55.6; HRMS (ESI) *m/z*: $[M + H]^+$ calculated for $C_{24}H_{16}N_3O_3^+$, 394.1186; found, 394.1143.

1,3-Dioxo-2-phenyl-2,3-dihydro-1*H*-benzo[*e*]pyrido[1',2':1,2]imidazo-[4,5-*g*]isoindole-5-carbonitrile (13da).

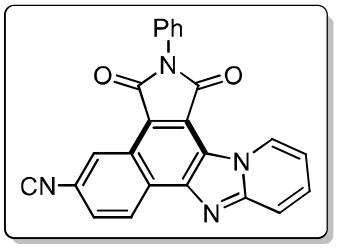

Purified by column chromatography using ethyl acetate/petroleum ether (7: 3 *v/v*) as eluent; yellow solid (68 mg, 77%); mp 289-291 ºC; ^{1}H NMR (400 MHz, $CDCl_3$) δ 10.21 (dt, *J* = 7.0, 1.2 Hz, 1H), 9.65 – 9.64 (m, 1H), 9.09 (dd, *J* = 8.6, 0.8 Hz, 1H), 8.05 – 8.00 (m, 2H), 7.76 (ddd, *J* = 9.2, 6.8, 1.3 Hz, 1H), 7.64 – 7.57 (m, 4H), 7.55 – 7.50 (m, 1H), 7.22 (td, *J* = 6.9, 1.2 Hz, 1H); ^{13}C{^{1}H} NMR (100 MHz, $CDCl_3$) δ 168.7, 167.6, 150.5, 136.1, 132.6, 131.6, 131.3, 130.6, 130.0, 129.5, 128.9, 128.6, 128.1, 126.4, 125.3, 125.0, 122.0, 119.6, 118.6, 117.9, 113.4, 112.4; HRMS (ESI) m/z: $[M + H]^+$ calculated for $C_{24}H_{13}N_4O_2^+$, 389.1033; found, 389.1069.

2-Phenyl-5-(trifluoromethyl)-1*H*-benzo[*e*]pyrido[1',2':1,2]imidazo[4,5-*g*]isoindole-1,3(2*H*)-dione (13ea).

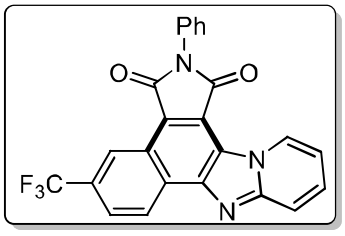

Purified by column chromatography using ethyl acetate/petroleum ether (6: 4 *v/v*) as eluent; yellow solid (68 mg, 83%); mp 309-311 ºC; ^{1}H NMR (400 MHz, $CDCl_3$) δ 10.14 (d, *J* = 7.0 Hz, 1H), 9.53 (s, 1H), 9.08 (d, *J* = 8.7 Hz, 1H), 8.06 (d, *J* = 8.7 Hz, 1H), 7.98 (d, *J* = 9.2 Hz, 1H), 7.72 (t, *J* = 8.0 Hz, 1H), 7.65 – 7.60 (m, 4H), 7.54 – 7.50 (m, 1H), 7.17 (t, *J* = 6.9 Hz, 1H); ^{13}C{^{1}H} NMR (100 MHz, $CDCl_3$) δ

168.1, 167.1, 150.5, 146.9, 131.5, 131.4, 130.5, 130.3, 129.3, 128.3, 126.8, 125.5, 124.9, 124.8, 124.7, 124.7, 123.5, 123.5, 121.4, 119.9, 117.9, 113.4; HRMS (ESI) *m/z*: $[M + H]^+$ calculated for $C_{24}H_{13}F_3N_3O_2^+$, 432.0954; found, 432.0916.

10-Methyl-2-phenyl-1*H*-benzo[*e*]pyrido[1',2':1,2]imidazo[4,5-*g*]isoindole-1,3(2*H*)-dione

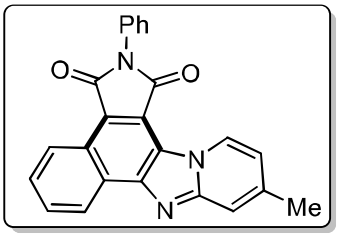

(13fa). Purified by column chromatography using ethyl acetate/petroleum ether (6: 4 *v/v*) as eluent; orange solid (68 mg, 75%); mp 272-274 ºC; ^{1}H NMR (400 MHz, $CDCl_3$) δ 9.97 (d, *J* = 7.1 Hz, 1H), 9.18 – 9.16 (m, 1H), 8.91 (d, *J* = 7.5 Hz, 1H), 7.83 (d, *J* = 5.8 Hz, 2H), 7.67 (s, 1H), 7.60 (d, *J* = 4.7 Hz, 3H), 7.53 – 7.50 (m, 2H), 6.91 (d, *J* = 7.6 Hz, 1H), 2.59 (s, 3H); ^{13}C{^{1}H} NMR (100 MHz, $CDCl_3$) δ 168.6, 167.7, 150.7, 147.6, 142.8, 131.7, 129.4, 129.2, 129.2, 128.8, 128.1, 126.9, 126.9, 126.5 , 125.7, 123.8, 120.0, 118.9, 116.0, 115.9, 115.5, 22.1; HRMS (ESI) *m/z*: $[M + H]^+$ calculated for $C_{24}H_{16}N_3O_2^+$, 378.1237; found, 378.1192.

11-Iodo-2-phenyl-1*H*-benzo[*e*]pyrido[1',2':1,2]imidazo[4,5-*g*]isoindole-1,3(2*H*)-dione (13ga).

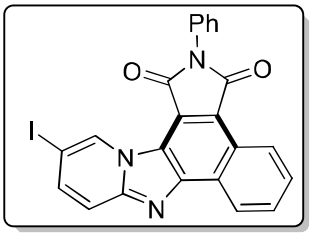

Purified by column chromatography using ethyl acetate/petroleum ether (6: 4 *v/v*) as eluent; yellow solid (49 mg, 64%); mp 257-259 ºC; ^{1}H NMR (400 MHz, $CDCl_3$) δ 10.40 (dd, *J* = 1.6, 1.2 Hz, 1H), 9.19 – 9.17 (m, 1H), 8.94 – 8.92 (m, 1H), 7.92 – 7.84 (m, 2H), 7.81 (dd, *J* = 9.2, 1.6 Hz, 1H), 7.74 (dd, *J* = 9.6, 1.2 Hz, 1H), 7.57 – 7.64 (m, 4H), 7.53 – 7.49 (m, 1H); ^{13}C{^{1}H} NMR (100 MHz, $CDCl_3$) δ 168.4, 167.6, 148.5, 146.9, 138.6, 135.1, 131.5, 129.4, 129.3, 129.2, 129.0, 128.4, 127.0, 126.5, 125.9, 123.8, 120.6, 120.1, 118.67, 118.4, 75.0; HRMS (ESI) *m/z*: $[M + H]^+$ calculated for $C_{23}H_{13}IN_3O_2^+$, 490.0047; found, 489.9990.

10-Methyl-5-nitro-2-phenyl-1*H*-benzo[*e*]pyrido[1',2':1,2]imidazo[4,5-*g*]isoindole-1,3(2*H*)-dione (13ha). Purified by column chromatography using ethyl acetate/petroleum ether (7: 3 *v/v*) as eluent; yellow solid (65 mg, 78%); mp 273-275 ºC; ^{1}H NMR (400 MHz, $CDCl_3$) δ 10.06 (d, *J* = 2.2 Hz, 1H), 10.00 (d, *J* = 7.1 Hz, 1H), 9.07 (d, *J* = 9.1 Hz, 1H), 8.60 (dd, *J* = 9.1, 2.3 Hz, 1H), 7.74 (s, 1H), 7.65 – 7.59 (m, 4H), 7.53 – 7.50 (m, 1H), 7.02 (d, *J* = 7.1 Hz, 1H), 2.63 (s, 3H); ^{13}C{^{1}H} NMR (100 MHz, $CDCl_3$) δ 165.6, 165.1, 151.5, 144.1, 133.4, 131.4, 131.3, 129.6, 129.3, 128.4, 126.7, 125.5, 124.5, 122.1,

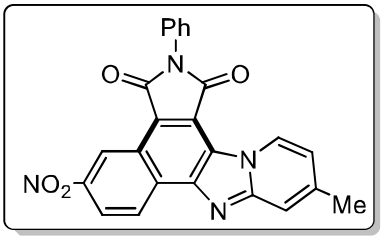

121.2, 119.8, 116.4, 116.3, 114.4, 114.1, 22.2; HRMS (ESI) *m/z*: $[M + H]^+$ calculated for $C_{24}H_{15}N_4O_4^+$, 423.1088; found, 423.1091.

7-Phenyl-6*H*-naphtho[2,3-*e*]pyrido[1',2':1,2]imidazo[4,5-*g*]isoindole-6,8(7*H*)-dione (13ia).

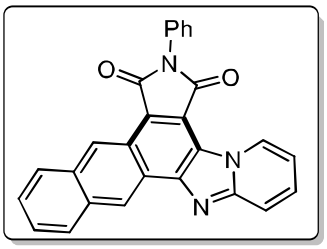

Purified by column chromatography using ethyl acetate/petroleum ether (6: 4 *v/v*) as eluent; red solid (51 mg, 61%); mp 301-303 ºC; ^{1}H NMR (400 MHz, $CDCl_3$) δ 10.12 (d, *J* = 6.9 Hz, 1H), 9.73 (s, 1H), 9.47 (s, 1H), 8.19 – 8.17 (m, 2H), 7.97 (d, *J* = 9.2 Hz, 1H), 7.66 – 7.60 (m, 7H), 7.53 – 7.49 (m, 1H), 7.12 (t, *J* = 6.9 Hz, 1H); ^{13}C{^{1}H} NMR (100 MHz, $CDCl_3$) δ 168.8, 167.7, 149.6, 147.6, 133.0, 132.9, 131.7, 130.2, 129.2, 129.2, 128.6, 128.0, 127.4, 126.8, 126.8, 126.3, 125.9, 123.9, 122.8, 121.7, 120.4, 117.6, 117.3, 115.5, 113.1; HRMS (ESI) *m/z*: $[M + H]^+$ calculated for $C_{27}H_{16}N_3O_2^+$, 414.1237; found, 414.1212.

2-Phenyl-1*H*-pyrido[2',1':2,3]imidazo[4,5-*e*]thieno[3,2-*g*]isoindole-1,3(2*H*)-dione (13ja).

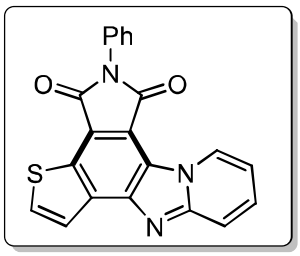

Purified by column chromatography using ethyl acetate/petroleum ether (6: 4 *v/v*) as eluent; red solid (52 mg, 56%); mp 300-302 ºC; ^{1}H NMR (400 MHz, $CDCl_3$) δ 10.12 (dt, *J* = 7.1, 1.2 Hz, 1H), 8.75 (d, *J* = 3.2 Hz, 1H), 8.58 (d, *J* = 3.2 Hz, 1H), 7.92 (d, *J* = 9.2 Hz, 1H), 7.64 – 7.55 (m, 4H), 7.51 – 7.45 (m, 2H), 7.13 (td, *J* = 6.8, 1.2 Hz, 1H); ^{13}C{^{1}H} NMR (100 MHz, $CDCl_3$) δ 168.3, 168.0, 149.5, 140.4, 133.0, 131.7, 130.0, 129.8, 129.5, 129.2, 128.0, 126.6, 121.6, 120.4, 119.7, 117.8, 117.6, 113.4, 100.0; HRMS (ESI) *m/z*: $[M + H]^+$ calculated for $C_{21}H_{12}N_3O_2S^+$, 370.0645; found, 370.0639.

5-Phenyl-4*H*-pyrido[2',1':2,3]imidazo[4,5-*e*]thieno[2,3-*g*]isoindole-4,6(5*H*)-dione (13ka).

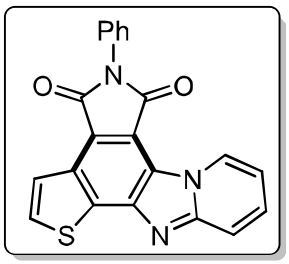

Purified by column chromatography using ethyl acetate/petroleum ether (6: 4 *v/v*) as eluent; yellow solid (65 mg, 71%); mp 240-242 ºC; ^{1}H NMR (400 MHz, $CDCl_3$) δ 10.17 (d, *J* = 7.1 Hz, 1H), 8.31 (d, *J* = 5.2 Hz, 1H), 7.92 – 7.88 (m, 2H), 7.68 (t, *J* = 8.0 Hz, 1H), 7.60 – 7.59 (m, 3H), 7.49 (d, *J* = 4 Hz, 2H), 7.11 (t, *J* = 6.9 Hz, 1H); ^{13}C{^{1}H} NMR (100 MHz, $CDCl_3$) δ 167.8, 167.7, 150.9, 144.8, 132.8, 131.7, 130.9, 130.6, 129.3, 129.2, 128.1, 126.8, 124.6, 122.8, 120.3, 118.8, 117.6, 112.5, 100.0; HRMS (ESI) *m/z*: $[M + H]^+$ calculated for $C_{21}H_{12}N_3O_2S^+$, 370.0645; found, 370.0639.

8-Phenylchromeno[4,3-*e*]pyrido[1',2':1,2]imidazo[4,5-*g*]isoindole-1,7,9(8*H*)-trione (13la).

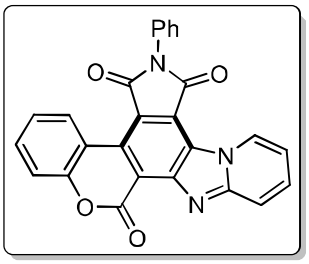

Purified by column chromatography using ethyl acetate/petroleum ether (6: 4 *v/v*) as eluent; brown solid (41 mg, 50%); mp 262-264 ºC; ^{1}H NMR (400 MHz, $CDCl_3$) δ 10.42 (d, *J* = 6.6 Hz, 1H), 9.33 (d, *J* = 8.2 Hz, 1H), 8.15 (s, 1H), 7.85 – 7.81 (m, 1H), 7.64 (t, *J* = 7.7 Hz, 3H), 7.58 – 7.54 (m, 3H), 7.51 (d, *J* = 8.4 Hz, 1H), 7.41 (t, *J* = 7.7 Hz, 1H), 7.20 (t, *J* = 8.0 Hz, 1H); ^{13}C{^{1}H} NMR (100 MHz, $CDCl_3$) δ 172.7, 170.7, 166.8, 151.7, 139.2, 134.4, 132.4, 131.6, 131.6, 131.2, 131.2, 130.3, 129.4, 128.9, 127.1, 125.9, 125.9, 118.9, 117.3, 116.1, 113.7, 112.5, 108.3; HRMS (ESI) *m/z*: $[M + H]^+$ calculated for $C_{26}H_{14}N_3O_4^+$, 432.0979; found, 432.0925.

2-Phenyl-1*H*-benzo[*e*]thiazolo[3',2':1,2]imidazo[4,5-*g*]isoindole-1,3(2*H*)-dione (13ma).

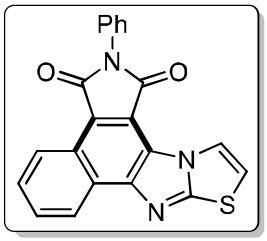

Purified by column chromatography using ethyl acetate/petroleum ether (6: 4 *v/v*) as eluent; yellow solid (48 mg, 52%); mp 194-196 ºC; ^{1}H NMR (100 MHz, $CDCl_3$) δ 9.17 – 9.14 (m, 1H), 8.79 (d, *J* = 4.5 Hz, 1H), 7.88 – 7.79 (m, 2H), 7.60 – 7.55 (m, 4H), 7.50 – 7.46 (m, 2H), 7.08 (d, *J* = 4.5 Hz, 1H); ^{13}C{^{1}H} NMR (100 MHz, $CDCl_3$) δ 168.8, 167.4, 138.7, 136.2, 134.8, 133.9, 133.4, 131.8, 131.3, 129.1, 128.0, 128.0, 126.7, 124.6, 123.0, 122.0, 118.2, 118.3, 112.1; HRMS (ESI) *m/z*: $[M + H]^+$ calculated for $C_{21}H_{12}N_3O_2S^+$, 370.0645; found, 370.0629.

2-Methyl-1*H*-benzo[*e*]pyrido[1',2':1,2]imidazo[4,5-*g*]isoindole-1,3(2*H*)-dione (13ab).

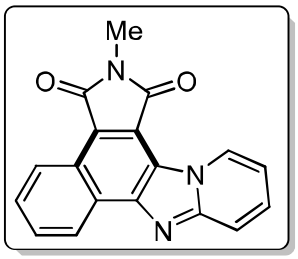

Purified by column chromatography using ethyl acetate/petroleum ether (7: 3 *v/v*) as eluent; yellow solid (67 mg, 80%); mp 297-299 ºC; ^{1}H NMR (400 MHz, $CDCl_3$) δ 10.01 (d, *J* = 6.9 Hz, 1H), 9.07 – 9.04 (m, 1H), 8.82 (d, *J* = 7.6 Hz, 1H), 7.89 (d, *J* = 9.2 Hz, 1H), 7.79 – 7.76 (m, 2H), 7.63 (t, *J* = 7.9 Hz, 1H), 7.10 (t, *J* = 6.8 Hz, 1H), 3.29 (s, 3H); ^{13}C{^{1}H} NMR (100 MHz, $CDCl_3$) δ 169.7, 168.4, 149.8, 130.6, 130.4, 128.7, 128.7, 128.6, 126.2, 125.5, 123.6, 123.6, 120.3, 118.8, 117.5, 112.7, 112.6, 23.9; HRMS (ESI) *m/z*: $[M + H]^+$ calculated for $C_{18}H_{12}N_3O_2^+$, 302.0924; found, 302.0936.

2,5-Dimethyl-1*H*-benzo[*e*]pyrido[1',2':1,2]imidazo[4,5-*g*]isoindole-1,3(2*H*)-dione (13bb).

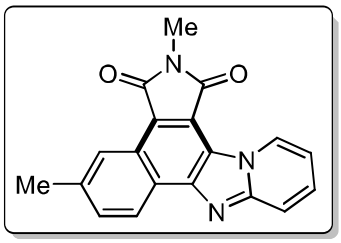

Purified by column chromatography using ethyl acetate/petroleum ether (7: 3 *v/v*) as eluent; yellow solid (54 mg, 71%); mp 206-208 ºC; ^{1}H NMR (400 MHz, $CDCl_3$) δ 10.11 (dt, *J* = 6.9, 1.2 Hz, 1H), 8.94 (s, 1H), 8.80 (d, *J* = 8.4 Hz, 1H), 7.92 (dt, *J* = 9.2, 1.2 Hz, 1H), 7.69 – 7.64 (m, 1H), 7.63 – 7.60 (m, 1H), 7.12 (td, *J* = 6.8, 1.2 Hz, 1H), 3.32 (s, 3H), 2.67 (s, 3H); ^{13}C{^{1}H} NMR (100 MHz, $CDCl_3$) δ 170.0, 168.7, 149.9, 139.1, 131.0, 130.7, 130.4, 130.2, 126.7, 124.7, 123.5, 120.4, 119.9, 118.7, 117.5, 112.5, 100.0, 24.0, 22.1; HRMS (ESI) *m/z*: $[M + H]^+$ calculated for $C_{19}H_{14}N_3O_2^+$, 316.1081; found, 316.1089.

5-Methoxy-2-methyl-1*H*-benzo[*e*]pyrido[1',2':1,2]imidazo[4,5-*g*]isoindole-1,3(2*H*)-dione

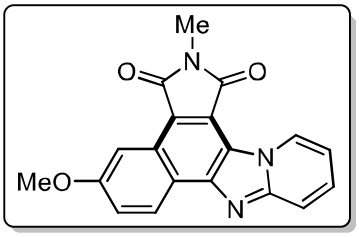

(13cb). Purified by column chromatography using ethyl acetate/petroleum ether (7: 3 *v/v*) as eluent; yellow solid (48 mg, 65%); mp 236-238 ºC; ^{1}H NMR (400 MHz, $CDCl_3$) δ 10.10 (d, *J* = 6.9 Hz, 1H), 8.79 (d, *J* = 9.1 Hz, 1H), 8.51 (d, *J* = 2.6 Hz, 1H), 7.89 (d, *J* = 9.1 Hz, 1H), 7.64 (ddd, *J* = 9.2, 6.7, 1.3 Hz, 1H), 7.46 (dd, *J* = 9.1, 2.6 Hz, 1H), 7.11 (td, *J* = 6.8, 1.2 Hz, 1H), 4.07 (s, 3H), 3.32 (s, 3H); ^{13}C{^{1}H} NMR (100 MHz, $CDCl_3$) δ 170.2, 168.6, 160.2, 130.8, 130.5, 128.2, 125.2, 123.9, 123.6, 122.8, 121.1, 120.5, 117.4, 112.4, 111.3, 105.0, 104.0, 55.6, 23.9; HRMS (ESI) *m/z*: $[M + H]^+$ calculated for $C_{19}H_{14}N_3O_3^+$, 332.1030; found, 332.1039.

2-Methyl-1,3-dioxo-2,3-dihydro-1*H*-benzo[*e*]pyrido[1',2':1,2]imidazo-[4,5-*g*]isoindole-5-carbonitrile (13db).

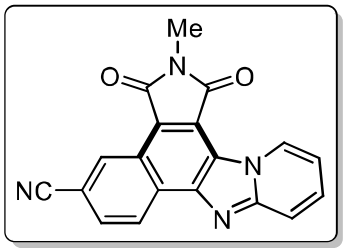

Purified by column chromatography using ethyl acetate/petroleum ether (7: 3 *v/v*) as eluent; yellow solid (58 mg, 78%); mp 203-205 ºC; ^{1}H NMR (400 MHz, $CDCl_3$) δ 10.15 (d, *J* = 7.0 Hz, 1H), 9.57 (d, *J* = 1.6 Hz, 1H), 9.03 (d, *J* = 8.6 Hz, 1H), 8.00 – 7.97 (m, 2H), 7.76 – 7.72 (m, 1H), 7.22 (td, *J* = 6.8, 1.2 Hz, 1H), 3.36 (s, 3H); ^{13}C{^{1}H} NMR (100 MHz, $CDCl_3$) δ 169.0, 168.0, 150.5, 146.4, 131.6, 131.3, 130.5, 130.0, 129.4, 125.3, 125.0, 122.1, 120.4, 119.8, 118.6, 118.0, 113.4, 112.4, 24.2; HRMS (ESI) *m/z*: $[M + H]^+$ calculated for $C_{19}H_{11}N_4O_2^+$, 327.0877; found, 327.0884.

7-Methyl-6*H*-naphtho[2,3-*e*]pyrido[1',2':1,2]imidazo[4,5-*g*]isoindole-6,8(7*H*)-dione (13hb).

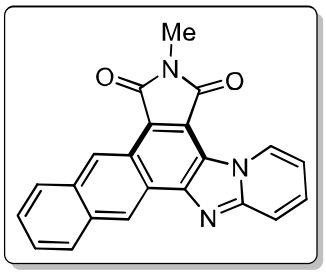

Purified by column chromatography using ethyl acetate/petroleum ether (7: 3 *v/v*) as eluent; red solid (44 mg, 62%); mp 222-224 ºC; ^{1}H NMR (400 MHz, $CDCl_3$) δ 10.12 (d, *J* = 6.9 Hz, 1H), 9.72 (s, 1H), 9.46 (s, 1H), 8.21 (t, *J* = 8.8 Hz, 2H), 7.97 (d, *J* = 9.1 Hz, 1H), 7.67 – 7.63 (m, 3H), 7.16 (t, *J* = 6.8 Hz, 1H), 3.34 (s, 3H); ^{13}C{^{1}H} NMR (100 MHz, $CDCl_3$) δ 172.9, 170.1, 158.7, 147.2, 143.2, 138.3, 132.8, 130.1, 130.0, 129.2, 128.6, 127.9, 127.3, 126.7, 125.7, 124.0, 122.7, 119.7, 117.6, 113.1, 100.0, 24.0; HRMS (ESI) *m/z*: $[M + H]^+$ calculated for $C_{22}H_{14}N_3O_2^+$, 352.1081; found, 352.1103.

2-Ethyl-1*H*-benzo[*e*]pyrido[1',2':1,2]imidazo[4,5-*g*]isoindole-1,3(2*H*)-dione (13ac). Purified

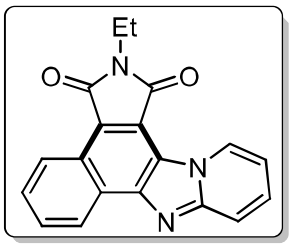

by column chromatography using ethyl acetate/petroleum ether (7: 3 *v/v*) as eluent; yellow solid (67 mg, 82%); mp 224-226 ºC; ^{1}H NMR (400 MHz, $CDCl_3$) δ 10.08 (dt, *J* = 6.9, 1.3 Hz, 1H), 9.12 – 9.10 (m, 1H), 8.88 – 8.85 (m, 1H), 7.90 (dt, *J* = 9.3, 1.2 Hz, 1H), 7.83 – 7.76 (m, 2H), 7.66 – 7.61 (m, 1H), 7.10 (td, *J* = 6.8, 1.2 Hz, 1H), 3.88 (q, *J* = 7.2 Hz, 2H), 1.41 (t, *J* = 7.2 Hz, 3H); ^{13}C{^{1}H} NMR (100 MHz, $CDCl_3$) δ 169.6, 168.4, 149.9, 146.7, 130.6, 130.4, 130.2, 128.7, 128.6, 126.3, 125.5, 123.6, 120.4, 120.3, 118.9, 117.6, 112.5, 33.0, 14.2; HRMS (ESI) *m/z*: $[M + H]^+$ calculated for $C_{19}H_{14}N_3O_2^+$, 316.1081; found, 316.1095.

2-Ethyl-5-methyl-1*H*-benzo[*e*]pyrido[1',2':1,2]imidazo[4,5-*g*]isoindole-1,3(2*H*)-dione (13bc).

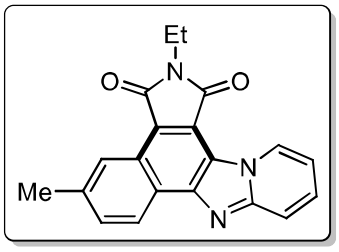

Purified by column chromatography using ethyl acetate/petroleum ether (7: 3 *v/v*) as eluent; yellow solid (55 mg, 69%); mp 282-284 ºC; ^{1}H NMR (400 MHz, $CDCl_3$) δ 10.16 (dt, *J* = 6.9, 1.2 Hz, 1H), 8.99 (s, 1H), 8.83 (d, *J* = 8.4 Hz, 1H), 7.93 (d, *J* = 9.3 Hz, 1H), 7.71 – 7.63 (m, 2H), 7.12 (td, *J* = 6.8, 1.2 Hz, 1H), 3.90 (q, *J* = 7.2 Hz, 2H), 2.68 (s, 3H), 1.40 (t, *J* = 7.2 Hz, 3H); ^{13}C{^{1}H} NMR (100 MHz, $CDCl_3$) δ 169.6, 168.3, 149.8, 146.7, 138.9, 130.7, 130.4, 130.4, 126.6, 126.5, 124.5, 123.3, 120.2, 119.6, 118.5, 117.4, 112.3, 32.9, 22.1, 14.2; HRMS (ESI) *m/z*: $[M + H]^+$ calculated for $C_{20}H_{16}N_3O_2^+$, 330.1237; found, 330.1250.

2-Ethyl-5-methoxy-1*H*-benzo[*e*]pyrido[1',2':1,2]imidazo[4,5-*g*]isoindole-1,3(2*H*)-dione

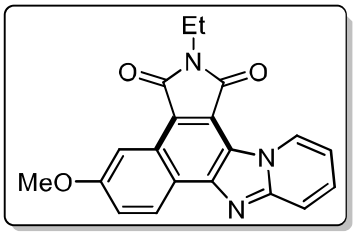

(13cc). Purified by column chromatography using ethyl acetate/petroleum ether (7: 3 *v/v*) as eluent; red solid (49 mg, 64%); mp 230-232 ºC; ^{1}H NMR (400 MHz, $CDCl_3$) δ 10.06 (d, *J* = 6.9 Hz, 1H), 8.73 (d, *J* = 9.1 Hz, 1H), 8.46 (d, *J* = 2.5 Hz, 1H), 7.88 (d, *J* = 9.1 Hz, 1H), 7.63 (t, *J* = 8.1 Hz, 1H), 7.41 (d, *J* = 9.1 Hz, 1H), 7.09 (t, *J* = 6.9 Hz, 1H), 4.05 (s, 3H), 3.87 (q, *J* = 7.2 Hz, 2H), 1.40 (t, *J* = 7.2 Hz, 3H); ^{13}C{^{1}H} NMR (100 MHz, $CDCl_3$) δ 169.9, 168.4, 160.2, 150.1, 147.0, 130.8, 130.5, 128.1, 125.1, 123.5, 121.1, 120.5, 118.8, 118.3, 117.3, 112.3, 103.9, 55.6, 33.0, 14.2; HRMS (ESI) *m/z*: $[M + H]^+$ calculated for $C_{20}H_{16}N_3O_3^+$, 346.1186; found, 346.1187.

2-Ethyl-1,3-dioxo-2,3-dihydro-1*H*-benzo[*e*]pyrido[1',2':1,2]imidazo-[4,5-*g*]isoindole-5-carbonitrile (13dc). Purified by column chromatography using ethyl acetate/petroleum ether (7: 3 *v/v*) as eluent; yellow solid (59 mg, 76%); mp 307-309 ºC; ^{1}H NMR (400 MHz, $CDCl_3$) δ 10.13 (d, *J* = 7.1 Hz, 1H), 9.54 (d, *J* = 1.6 Hz, 1H), 9.00 (d, *J* = 8.6 Hz, 1H), 7.99 – 7.95 (m, 2H), 7.76 – 7.71 (m, 1H), 7.21 (td, *J* = 6.8, 1.2 Hz, 1H), 3.92 (q, *J* = 7.2 Hz, 2H), 1.43 (t, *J* = 7.2 Hz, 3H); ^{13}C{^{1}H} NMR (100 MHz, $CDCl_3$) δ 168.8, 167.8, 150.5, 131.5, 131.3, 130.6, 130.0, 129.7, 129.4, 126.0, 125.3, 124.9, 122.1, 119.8, 118.7, 117.9, 113.4, 112.3, 33.3, 14.1; HRMS (ESI) *m/z*: $[M + H]^+$ calculated for $C_{20}H_{13}N_4O_2^+$, 341.1033; found, 341.1039.

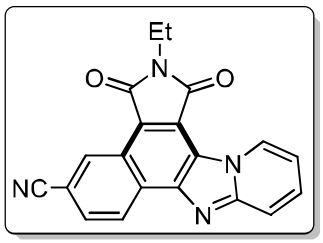

2-Ethyl-1*H*-pyrido[2',1':2,3]imidazo[4,5-*e*]thieno[3,2-*g*]isoindole-1,3(2*H*)-dione (13ic).

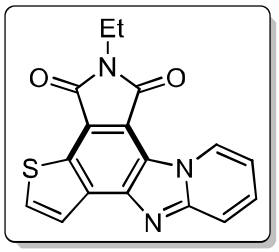

Purified by column chromatography using ethyl acetate/petroleum ether (7: 3 *v/v*) as eluent; yellow solid (41 mg, 51%); mp 293-295 ºC; ^{1}H NMR (400 MHz, $CDCl_3$) δ 10.10 (dt, *J* = 6.9, 1.2 Hz, 1H), 8.19 (d, *J* = 5.4 Hz, 1H), 7.97 (d, *J* = 5.4 Hz, 1H), 7.89 (dt, *J* = 9.2, 1.2 Hz, 1H), 7.69 – 7.64 (m, 1H), 7.11 (td, *J* = 6.8, 1.2 Hz, 1H), 3.90 (q, *J* = 7.2 Hz, 2H), 1.41 (t, *J* = 7.2 Hz, 3H); ^{13}C{^{1}H} NMR (100 MHz, $CDCl_3$) δ 168.5, 168.3, 150.4, 136.0, 133.0, 132.7, 131.4, 131.0, 130.6, 123.2, 121.5, 117.6, 114.8, 114.6, 112.3, 33.2, 14.2; HRMS (ESI) *m/z*: $[M + H]^+$ calculated for $C_{17}H_{12}N_3O_2S^+$, 322.0645; found, 322.0636.

2-Benzyl-1*H*-benzo[*e*]pyrido[1',2':1,2]imidazo[4,5-*g*]isoindole-1,3(2*H*)-dione (13ad). Purified

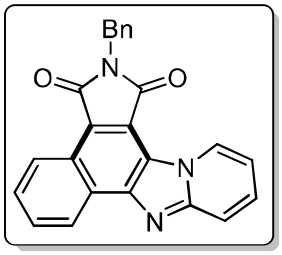

by column chromatography using ethyl acetate/petroleum ether (7: 3 *v/v*) as eluent; red solid (65 mg, 67%); mp 208-210 ºC; ^{1}H NMR (400 MHz, $CDCl_3$) δ 10.12 (dt, *J* = 6.9, 1.2 Hz, 1H), 9.18 – 9.14 (m, 1H), 8.92 – 8.88 (m, 1H), 7.91 (dt, *J* = 9.2, 1.2 Hz, 1H), 7.85 – 7.79 (m, 2H), 7.64 (ddd, *J* = 9.2, 6.8, 1.4 Hz, 1H), 7.56 – 7.53 (m, 2H), 7.40 – 7.36 (m, 2H), 7.33 – 7.30 (m, 1H), 7.11 (td, *J* = 6.9, 1.2 Hz, 1H), 5.00 (s, 2H); ^{13}C{^{1}H} NMR (100 MHz, $CDCl_3$) δ 169.5, 168.3, 150.0, 147.0, 136.6, 130.8, 130.5, 128.9, 128.8, 128.5, 127.9, 126.4, 125.6, 123.7, 120.4, 120.2, 119.0, 117.6, 112.6, 41.7; HRMS (ESI) *m/z*: $[M + H]^+$ calculated for $C_{24}H_{16}N_3O_2^+$, 378.1237; found, 378.1245.

2-Benzyl-5-methoxy-1*H*-benzo[*e*]pyrido[1',2':1,2]imidazo[4,5-*g*]isoindole-1,3(2*H*)-dione

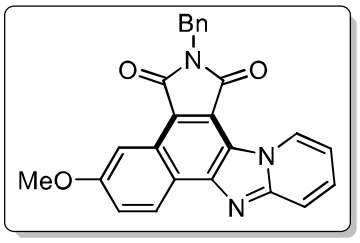

(13cd). Purified by column chromatography using ethyl acetate/petroleum ether (7: 3 *v/v*) as eluent; red solid (54 mg, 59%); mp 202-204 ºC; ^{1}H NMR (400 MHz, $CDCl_3$) δ 10.08 (dt, *J* = 6.9, 1.2 Hz, 1H), 8.77 (d, *J* = 9.0 Hz, 1H), 8.50 (d, *J* = 2.6 Hz, 1H), 7.87 (dt, *J* = 9.2, 1.2 Hz, 1H), 7.63 (ddd, *J* = 9.2, 6.7, 1.3 Hz, 1H), 7.55 – 7.53 (m, 2H), 7.45 (dd, *J* = 9.1, 2.6 Hz, 1H), 7.40 – 7.36 (m, 2H), 7.33 – 7.31 (m, 1H), 7.08 (td, *J* = 6.9, 1.2 Hz, 1H), 4.99 (s, 2H), 4.06 (s, 3H); ^{13}C{^{1}H} NMR (100 MHz, $CDCl_3$) δ 169.8, 168.3, 160.2, 150.3, 147.3, 136.6, 130.9, 130.6, 128.8, 128.4, 128.2, 127.9, 125.2, 123.7, 121.2, 120.4, 118.7, 118.4, 117.4, 112.4, 104.0, 55.6, 41.7; HRMS (ESI) *m/z*: $[M + H]^+$ calculated for $C_{25}H_{18}N_3O_3^+$, 408.1343; found, 408.1346.

2-Benzyl-1,3-dioxo-2,3-dihydro-1*H*-benzo[*e*]pyrido[1',2':1,2]imidazo-[4,5-*g*]isoindole-5-

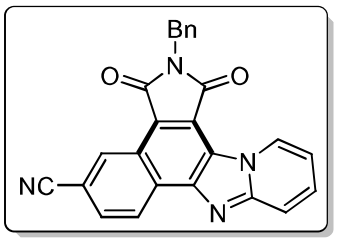

carbonitrile (13dd). Purified by column chromatography using ethyl acetate/petroleum ether (7: 3 *v/v*) as eluent; yellow solid (64 mg, 70%); mp 228-230 ºC; ^{1}H NMR (400 MHz, $CDCl_3$) δ 10.13 (dt, *J* = 7.0, 1.2 Hz, 1H), 9.56 (dd, *J* = 1.6, 0.7 Hz, 1H), 8.99 (dd, *J* = 8.6, 0.7 Hz, 1H), 7.98 – 7.94 (m, 2H), 7.75 – 7.70 (m, 1H), 7.56 – 7.54 (m, 2H), 7.21 – 7.38 (m, 2H), 7.35 – 7.32 (m, 1H), 7.20 (td, *J* = 6.9, 1.2 Hz, 1H), 5.02 (s, 2H); ^{13}C{^{1}H} NMR (100 MHz, $CDCl_3$) δ 168.7, 167.6, 136.1, 131.8, 131.6, 131.4, 131.3, 130.6, 129.5,

129.3, 128.9, 128.6, 128.1, 126.7, 125.3, 124.9, 122.0, 119.6, 118.6, 117.9, 113.4, 112.4, 41.9; HRMS (ESI) *m/z*: $[M + H]^+$ calculated for $C_{25}H_{15}N_4O_2^+$, 403.1190; found, 403.1188.

11-Iodo-2-phenyl-3*a*,13*b*-dihydro-1*H*-benzo[*e*]pyrido[1',2':1,2]-imidazo[4,5-*g*]isoindole-1,3(2*H*)-dione (14ga). Purified by column chromatography using ethyl acetate/petroleum ether (7: 3 *v/v*) as eluent; yellow solid (12 mg, 15%); mp 273-275 ºC; ^{1}H NMR (400 MHz, $CDCl_3$) δ 9.12 (s, 1H), 8.16 (dd, *J* = 7.6, 1.6 Hz, 1H), 7.78 (d, *J* = 7.6 Hz, 1H), 7.52 – 7.40 (m, 7H), 7.30 – 7.28 (m, 2H), 4.99 (d, *J* = 10.4 Hz, 1H), 4.80 (d, *J* = 10.4 Hz, 1H); ^{13}C{^{1}H} NMR (100 MHz, $CDCl_3$) δ 175.1, 174.0, 146.1, 140.1, 133.6, 131.4, 130.6, 130.0, 129.3, 129.1, 129.0, 128.7, 128.6, 127.1, 126.4, 123.3, 118.3, 111.2, 75.7, 44.2, 39.2; HRMS (ESI) *m/z*: $[M + H]^+$ calculated for $C_{23}H_{15}IN_3O_2^+$, 492.0203; found, 492.0155.

3.3A.4.4 X-ray Crystallographic Analysis of 13ac

The single crystals of the compound **13ac** were obtained as yellow color needles. The crystal data collection and data reduction were performed using CrysAlis PRO on a single crystal Rigaku Oxford XtaLab Pro diffractometer. The crystals were kept at 93(2) K during data collection using CuKα (λ = 1.54184) radiation. Using Olex2,[64] the structure was solved with the ShelXT[65] structure solution program using Intrinsic Phasing and refined with the ShelXL[66] refinement package using Least Squares minimization.

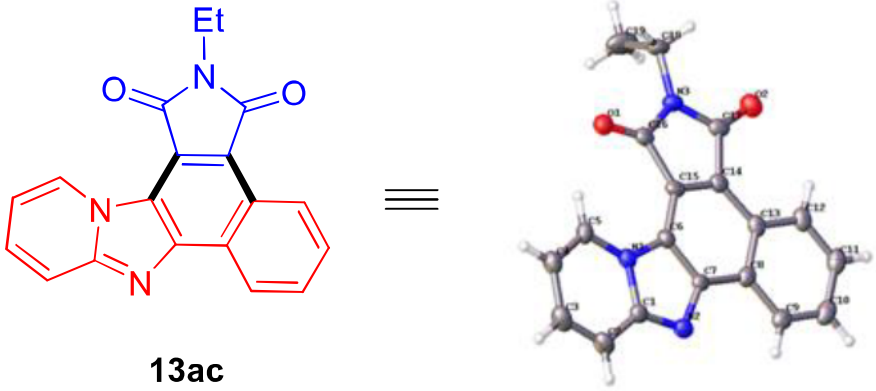

13ac

Table 3.3A.4 Crystal data and structure refinement for **13ac (exp-562-AK-VNS-848).**

Identification code	Exp-562-AK-VNS-848
Empirical formula	$C_{19}H_{13}N_3O_2$
Formula weight	315.32
Temperature/K	93(2)
Crystal system	monoclinic
Space group	$P2_1/n$
a/Å	6.96200(10)
b/Å	11.9742(2)
c/Å	17.6301(3)
α/°	90
β/°	96.3520(10)
γ/°	90
Volume/Å^3	1460.70(4)
Z	4
ρ_{calc}g/cm^3	1.434
μ/mm^{-1}	0.779
F(000)	656.0
Crystal size/mm^3	0.2 × 0.07 × 0.05
Radiation	CuKα (λ = 1.54184)
2Θ range for data collection/°	8.944 to 159.792
Index ranges	$-7 \leq h \leq 8$, $-12 \leq k \leq 14$, $-22 \leq l \leq 22$
Reflections collected	8409
Independent reflections	3091 [R_{int} = 0.0303, R_{sigma} = 0.0361]
Data/restraints/parameters	3091/0/218
Goodness-of-fit on F^2	1.054
Final R indexes [I>=2σ (I)]	R_1 = 0.0545, wR_2 = 0.1429
Final R indexes [all data]	R_1 = 0.0584, wR_2 = 0.1461
Largest diff. peak/hole / e Å^{-3}	0.60/-0.22

3.3A.5 REFERENCES

1. Arndtsen, B. A.; Bergman, R. G.; Mobley, T. A.; Peterson, T. H., *Accounts of Chemical Research* **1995,** *28*, 154-162.
2. Ardkhean, R.; Caputo, D.; Morrow, S.; Shi, H.; Xiong, Y.; Anderson, E., *Chemical Society Reviews* **2016,** *45*, 1557-1569.
3. Tietze, L. F., *Chemical Reviews* **1996,** *96*, 115-136.

4. Kroutil, W.; Rueping, M., I*ntroduction to ACS Catalysis Virtual Special Issue on Cascade Catalysis. ACS Publications*: **2014**.
5. Baccalini, A.; Faita, G.; Zanoni, G.; Maiti, D., *Chemistry–A European Journal* **2020,** *26*, 9749-9783.
6. Peneau, A.; Guillou, C.; Chabaud, L., *European Journal of Organic Chemistry* **2018,** *2018*, 5777-5794.
7. Ackermann, L., *Chemical Reviews* **2011,** *111*, 1315-1345.
8. Gorelsky, S. I.; Lapointe, D.; Fagnou, K., *Journal of the American Chemical Society* **2008,** *130*, 10848-10849.
9. Thiyagarajan, S.; Gunanathan, C., *ACS Catalysis* **2018,** *8*, 2473-2478.
10. Tan, X.; Gao, S.; Zeng, W.; Xin, S.; Yin, Q.; Zhang, X., *Journal of the American Chemical Society* **2018,** *140*, 2024-2027.
11. Liang, T.; Tan, Z.; Zhao, H.; Chen, X.; Jiang, H.; Zhang, M., *ACS Catalysis* **2018,** *8*, 2242-2246.
12. Sakamoto, R.; Kato, T.; Sakurai, S.; Maruoka, K., *Organic Letters* **2018,** *20*, 1400-1403.
13. Ueno, R.; Natsui, S.; Chatani, N., *Organic Letters* **2018,** *20*, 1062-1065.
14. Manan, R. S.; Zhao, P., *Nature Communications* **2016,** *7*, 1-11.
15. Sun, T.; Zhang, Y.; Qiu, B.; Wang, Y.; Qin, Y.; Dong, G.; Xu, T., *Angewandte Chemie* **2018,** *130*, 2909-2913.
16. Wu, X.; Xiong, H.; Sun, S.; Cheng, J., *Organic Letters* **2018,** *20*, 1396-1399.
17. Grenet, E.; Waser, J., *Organic Letters* **2018,** *20*, 1473-1476.
18. Kumar, S.; Vasantha, V., *Organic Chemistry Frontiers* **2018,** *5*, 2630-2635.
19. Yang, Y.; Li, K.; Cheng, Y.; Wan, D.; Li, M.; You, J., *Chemical Communications* **2016,** *52*, 2872-2884.
20. Satoh, T.; Miura, M., *Chemistry–A European Journal* **2010,** *16*, 11212-11222.
21. Lhassani, M.; Chavignon, O.; Chezal, J. M.; Teulade, J. C.; Chapat, J. P.; Snoeck, R.; Andrei, G.; Balzarini, J.; De Clercq, E.; Gueiffier, A., *European Journal of Medicinal Chemistry* **1999,** *34*, 271-274.
22. Badawey, E.; Kappe, T., *European Journal of Medicinal Chemistry* **1995,** *30*, 327-332.
23. Rupert, K. C.; Henry, J. R.; Dodd, J. H.; Wadsworth, S. A.; Cavender, D. E.; Olini, G. C.; Fahmy, B.; Siekierka, J. J., *Bioorganic & Medicinal Chemistry Letters* **2003,** *13*, 347-350.

24. Kaminski, J. J.; Doweyko, A. M., *Journal of Medicinal Chemistry* **1997,** *40*, 427-436.
25. Langer, S.; Arbilla, S.; Benavides, J.; Scatton, B., *Advances in Biochemical Psychopharmacology* **1990,** *46*, 61-72.
26. Mizushige, K.; Ueda, T.; Yukiiri, K.; Suzuki, H., *Cardiovascular Drug Reviews* **2002,** *20*, 163-174.
27. Almirante, L.; Polo, L.; Mugnaini, A.; Provinciali, E.; Rugarli, P.; Biancotti, A.; Gamba, A.; Murmann, W., *Journal of Medicinal Chemistry* **1965,** *8*, 305-312.
28. Budke, B.; Kalin, J. H.; Pawlowski, M.; Zelivianskaia, A. S.; Wu, M.; Kozikowski, A. P.; Connell, P. P., *Journal of Medicinal Chemistry* **2013,** *56*, 254-263.
29. Bin, J. W.; Wong, I. L.; Hu, X.; Yu, Z. X.; Xing, L. F.; Jiang, T.; Chow, L. M.; Biao, W. S., *Journal of Medicinal Chemistry* **2013,** *56*, 9057-9070.
30. Horenstein, N. A.; Papke, R. L., *Anti-inflammatory Silent Agonists. ACS Publications*: 2017.
31. Sato, M.; Dander, J. E.; Sato, C.; Hung, Y. S.; Gao, S. S.; Tang, M. C.; Hang, L.; Winter, J. M.; Garg, N. K.; Watanabe, K., *Journal of the American Chemical Society* **2017,** *139*, 5317-5320.
32. Zheng, K.; Chen, Y.; Wang, J.; Zheng, L.; Hutchinson, M.; Persson, J.; Ji, J., *Journal of Pharmaceutical Sciences* **2019,** *108*, 133-141.
33. Li, P.; Zhang, X.; Fan, X., *The Journal of Organic Chemistry* **2015,** *80*, 7508-7518.
34. Qi, Z.; Yu, S.; Li, X., *The Journal of Organic Chemistry* **2015,** *80*, 3471-3479.
35. Peng, H.; Yu, J.-T.; Jiang, Y.; Wang, L.; Cheng, J., *Organic & Biomolecular Chemistry* **2015,** *13*, 5354-5357.
36. Kotla, S. K. R.; Choudhary, D.; Tiwari, R. K.; Verma, A. K., *Tetrahedron Letters* **2015,** *56*, 4706-4710.
37. Wang, W.; Niu, J. L.; Liu, W. B.; Shi, T. H.; Hao, X. Q.; Song, M. P., *Tetrahedron* **2015,** *71*, 8200-8207.
38. Ghosh, M.; Naskar, A.; Mishra, S.; Hajra, A., *Tetrahedron Letters* **2015,** *56*, 4101-4104.
39. Meena, N.; Sharma, S.; Bhatt, R.; Shinde, V. N.; Sunda, A. P.; Bhuvanesh, N.; Kumar, A.; Joshi, H., *Chemical Communications* **2020,** *56*, 10223-10226.
40. Zheng, G.; Tian, M.; Xu, Y.; Chen, X.; Li, X., *Organic Chemistry Frontiers* **2018,** *5*, 998-1002.

41. Reddy, K. N.; Chary, D. Y.; Sridhar, B.; Reddy, B. S., *Organic Letters* **2019,** *21*, 8548-8552.
42. Ghosh, K.; Nishii, Y.; Miura, M., *Organic Letters* **2020,** *22*, 3547-3550.
43. Li, B.; Guo, C.; Shen, N.; Zhang, X.; Fan, X., *Organic Chemistry Frontiers* **2020,** *7*, 3698-3704.
44. Chary, D. Y.; Reddy, K. N.; Sridhar, B.; Reddy, B. S., *Tetrahedron Letters* **2021,** *66*, 152830.
45. Ackermann, L., *Chemical Reviews* **2011,** *111*, 1315-1345.
46. Ackermann, L.; Lygin, A. V.; Hofmann, N., *Angewandte Chemie International Edition* **2011,** *50*, 6379-6382.
47. Guo, C.; Li, B.; Liu, H.; Zhang, X.; Zhang, X.; Fan, X., *Organic Letters* **2019,** *21*, 7189-7193.
48. Seoane, A.; Casanova, N.; Quiñones, N.; Mascareñas, J. L.; Gulías, M., *Journal of the American Chemical Society* **2014,** *136*, 7607-7610.
49. Zhou, M. B.; Pi, R.; Hu, M.; Yang, Y.; Song, R. J.; Xia, Y.; Li, J. H., *Angewandte Chemie International Edition* **2014,** *53*, 11338-11341.
50. Volpi, G.; Garino, C.; Conterosito, E.; Barolo, C.; Gobetto, R.; Viscardi, G., *Dyes and Pigments* **2016,** *128*, 96-100.
51. Firmansyah, D.; Banasiewicz, M.; Deperasińska, I.; Makarewicz, A.; Kozankiewicz, B.; Gryko, D. T., *Chemistry – An Asian Journal* **2014,** *9*, 2483-2493.
52. Firmansyah, D.; Banasiewicz, M.; Gryko, D. T., *Organic & Biomolecular Chemistry* **2015,** *13*, 1367-1374.
53. Banasiewicz, M.; Deperasinska, I.; Makarewicz, A.; Firmansyah, D.; Gryko, D. T.; Kozankiewicz, B., *Physical Chemistry Chemical Physics* **2015,** *17*, 8945-8950.
54. Nandwana, N. K.; Dhiman, S.; Shinde, V. N.; Beifuss, U.; Kumar, A., *European Journal of Organic Chemistry* **2020**, 2576–2582.
55. Yanai, T.; Tew, D. P.; Handy, N. C., *Chemical Physics Letters* **2004,** *393*, 51-57.
56. Krishnan, R.; Binkley, J. S.; Seeger, R.; Pople, J. A., *The Journal of Chemical Physics* **1980,** *72*, 650-654.
57. Zhao, Y.; Truhlar, D. G., *Accounts of Chemical Research* **2008,** *41*, 157-167.

58. Tomasi, J.; Cammi, R.; Mennucci, B.; Cappelli, C.; Corni, S., *Physical Chemistry Chemical Physics* **2002,** *4*, 5697-5712.

59. Frisch, M. J.; Trucks, G. W.; Schlegel, H. B.; Scuseria, G. E.; Robb, M. A.; Cheeseman, J. R.; Scalmani, G.; Barone, V.; Petersson, G. A.; Nakatsuji, H.; Li, X.; Caricato, M.; Marenich, A. V.; Bloino, J.; Janesko, B. G.; Gomperts, R.; Mennucci, B.; Hratchian, H. P.; Ortiz, J. V.; Izmaylov, A. F.; Sonnenberg, J. L.; Williams; Ding, F.; Lipparini, F.; Egidi, F.; Goings, J.; Peng, B.; Petrone, A.; Henderson, T.; Ranasinghe, D.; Zakrzewski, V. G.; Gao, J.; Rega, N.; Zheng, G.; Liang, W.; Hada, M.; Ehara, M.; Toyota, K.; Fukuda, R.; Hasegawa, J.; Ishida, M.; Nakajima, T.; Honda, Y.; Kitao, O.; Nakai, H.; Vreven, T.; Throssell, K.; Montgomery Jr., J. A.; Peralta, J. E.; Ogliaro, F.; Bearpark, M. J.; Heyd, J. J.; Brothers, E. N.; Kudin, K. N.; Staroverov, V. N.; Keith, T. A.; Kobayashi, R.; Normand, J.; Raghavachari, K.; Rendell, A. P.; Burant, J. C.; Iyengar, S. S.; Tomasi, J.; Cossi, M.; Millam, J. M.; Klene, M.; Adamo, C.; Cammi, R.; Ochterski, J. W.; Martin, R. L.; Morokuma, K.; Farkas, O.; Foresman, J. B.; Fox, D. J., *Gaussian 16 Rev. A.03*. Wallingford, CT, 2016.

60. Peng, X.; Song, F.; Lu, E.; Wang, Y.; Zhou, W.; Fan, J.; Gao, Y., *Journal of the American Chemical Society* **2005,** *127*, 4170-4171.

61. Takizawa, S. Y.; Nishida, J. I.; Tsuzuki, T.; Tokito, S.; Yamashita, Y., *Inorganic chemistry* **2007,** *46*, 4308-4319.

62. Williams, A. T. R.; Winfield, S. A.; Miller, J. N., *Analyst* **1983,** *108*, 1067-1071.

63. Fery-Forgues, S.; Lavabre, D., *Journal of Chemical Education* **1999,** *76*, 1260-1264.

64. Dolomanov, O. V.; Bourhis, L. J.; Gildea, R. J.; Howard, J. A. K.; Puschmann, H., *Journal of Applied Crystallography* **2009,** *42*, 339-341.

65. Sheldrick, G., *Acta Crystallographica Section A* **2015,** *71*, 3-8.

66. Sheldrick, G., *Acta Crystallographica Section C* **2015,** *71*, 3-8.